Galvin JE, Lee VM, Trojanowski JQ (2001) Synucleinopathies: clinical and pathological implications. Arch Neurol 58:186–190. CrossRef Medline

Garcia-Reitböck P, Anichtchik O, Bellucci A, Iovino M, Ballini C, Fineberg E, Ghetti B, Della Corte L, Spano P, Tofaris GK, Goedert M, Spillantini MG (2010) SNARE protein redistribution and synaptic failure in a transgenic mouse model of Parkinson's disease. Brain 133:2032–2044. CrossRef Medline

Gerfen CR, Surmeier DJ (2011) Modulation of striatal projection systems by dopamine. Annu Rev Neurosci 34:441–466. CrossRef Medline

Gimbel DA, Nygaard HB, Coffey EE, Gunther EC, Laurén J, Gimbel ZA, Strittmatter SM (2010) Memory Impairment in transgenic Alzheimer mice requires cellular prion protein. J Neurosci 30:6367–6374. CrossRef Medline

Gureviciene I, Gurevicius K, Tanila H (2007) Role of alpha-synuclein in synaptic glutamate release. Neurobiol Dis 28:83–89. CrossRef Medline

Haucke V, Neher E, Sigrist SJ (2011) Protein scaffolds in the coupling of synaptic exocytosis and endocytosis. Nat Rev Neurosci 12:127–138. CrossRef Medline

Hayes NVL, Baines AJ (1996) Small synaptic vesicles. In: Biomembranes: a multi-volume treatise (Lee AG, ed), pp 75–122. Greenwich, CT: JAI.

Herzig MC, Kolly C, Persohn E, Theil D, Schweizer T, Hafner T, Stemmelen C, Troxler TJ, Schmid P, Danner S, Schnell CR, Mueller M, Kinzel B, Grevot A, Bolognani F, Stirn M, Kuhn RR, Kaupmann K, van der Putten PH, Rovelli G, et al. (2011) LRRK2 protein levels are determined by kinase function and are crucial for kidney and lung homeostasis in mice. Hum Mol Genet 20:4209–4223. CrossRef Medline

Hu K, Carroll J, Rickman C, Davletov B (2002) Action of Complexin on SNARE complex. J Biol Chem 277:41652–41656. CrossRef Medline

Iwai A, Masliah E, Yoshimoto M, Ge N, Flanagan L, de Silva HA, Kittel A, Saitoh T (1995) The precursor protein of non-A beta component of Alzheimer's disease amyloid is a presynaptic protein of the central nervous system. Neuron 14:467–475. CrossRef Medline

Iwasaki S, Kataoka M, Sekiguchi M, Shimazaki Y, Sato K, Takahashi M (2000) Two distinct mechanisms underlie the stimulation of neurotransmitter release by phorbol esters in clonal rat pheochromocytoma PC12 cells. J Biochem 128:407–414. CrossRef Medline

Kataoka M, Yamamori S, Suzuki E, Watanabe S, Sato T, Miyaoka H, Azuma S, Ikegami S, Kuwahara R, Suzuki-Migishima R, Nakahara Y, Nihonmatsu I, Inokuchi K, Katoh-Fukui Y, Yokoyama M, Takahashi M (2011) A single amino acid mutation in SNAP-25 induces anxiety-related behavior in mouse. PLoS One 6:e25158. CrossRef Medline

Kaushal N, Seminerio MJ, Shaikh J, Medina MA, Mesangeau C, Wilson LL, McCurdy CR, Matsumoto RR (2011) CM156, a high affinity sigma ligand, attenuates the stimulant and neurotoxic effects of methamphetamine in mice. Neuropharmacology 61:992–1000. CrossRef Medline

Kawamura Y, Fukaya M, Maejima T, Yoshida T, Miura E, Watanabe M, Ohno-Shosaku T, Kano M (2006) The CB_1 cannabinoid receptor is the major cannabinoid receptor at excitatory presynaptic sites in the hippocampus and cerebellum. J Neurosci 26:2991–3001. CrossRef Medline

Kramer ML, Schulz-Schaeffer WJ (2007) Presynaptic α-synuclein aggregates, not Lewy bodies, cause neurodegeneration in dementia with Lewy bodies. J Neurosci 27:1405–1410. CrossRef Medline

Kuwahara T, Koyama A, Koyama S, Yoshina S, Ren CH, Kato T, Mitani S, Iwatsubo T (2008) A systematic RNAi screen reveals involvement of endocytic pathway in neuronal dysfunction in alpha-synuclein transgenic C. elegans. Hum Mol Genet 17:2997–3009. CrossRef Medline

Larsen KE, Schmitz Y, Troyer MD, Mosharov E, Dietrich P, Quazi AZ, Savalle M, Nemani V, Chaudhry FA, Edwards RH, Stefanis L, Sulzer D (2006) α-Synuclein overexpression in PC12 and chromaffin cells impairs catecholamine release by interfering with a late step in exocytosis. J Neurosci 26:11915–11922. CrossRef Medline

Majewski H, Iannazzo L (1998) Protein kinase C: a physiological mediator of enhanced transmitter output. Prog Neurobiol 55:463–475. CrossRef Medline

Maroteaux L, Campanelli JT, Scheller RH (1988) Synuclein: a neuron-specific protein localized to the nucleus and presynaptic nerve terminal. J Neurosci 8:2804–2815. Medline

Masliah E, Rockenstein E, Veinbergs I, Sagara Y, Mallory M, Hashimoto M, Mucke L (2001) beta-amyloid peptides enhance alpha-synuclein accumulation and neuronal deficits in a transgenic mouse model linking Alzheimer's disease and Parkinson's disease. Proc Natl Acad Sci U S A 98:12245–12250. CrossRef Medline

McFarland MA, Ellis CE, Markey SP, Nussbaum RL (2008) Proteomics analysis identifies phosphorylation-dependent alpha-synuclein protein interactions. Mol Cell Proteomics 7:2123–2137. CrossRef Medline

Miyazaki T, Fukaya M, Shimizu H, Watanabe M (2003) Subtype switching of vesicular glutamate transporters at parallel fibre-Purkinje cell synapses in developing mouse cerebellum. Eur J Neurosci 17:2563–2572. CrossRef Medline

Morgan A, Burgoyne RD, Barclay JW, Craig TJ, Prescott GR, Ciufo LF, Evans GJ, Graham ME (2005) Regulation of exocytosis by protein kinase C. Biochem Soc Trans 33:1341–1344. CrossRef Medline

Morgan JR, Prasad K, Hao W, Augustine GJ, Lafer EM (2000) A conserved clathrin assembly motif essential for synaptic vesicle endocytosis. J Neurosci 20:8667–8676. Medline

Murphy DD, Rueter SM, Trojanowski JQ, Lee VM (2000) Synucleins are developmentally expressed, and α-synuclein regulates the size of the presynaptic vesicular pool in primary hippocampal neurons. J Neurosci 20:3214–3220. Medline

Nagy G, Matti U, Nehring RB, Binz T, Rettig J, Neher E, Sørensen JB (2002) Protein kinase C-dependent phosphorylation of synaptosome-associated protein of 25 kDa at Ser187 potentiates vesicle recruitment. J Neurosci 22:9278–9286. Medline

Nemani VM, Lu W, Berge V, Nakamura K, Onoa B, Lee MK, Chaudhry FA, Nicoll RA, Edwards RH (2010) Increased expression of alpha-synuclein reduces neurotransmitter release by inhibiting synaptic vesicle reclustering after endocytosis. Neuron 65:66–79. CrossRef Medline

Neumann M, Kahle PJ, Giasson BI, Ozmen L, Borroni E, Spooren W, Müller V, Odoy S, Fujiwara H, Hasegawa M, Iwatsubo T, Trojanowski JQ, Kretzschmar HA, Haass C (2002) Misfolded proteinase K-resistant hyperphosphorylated alpha-synuclein in aged transgenic mice with locomotor deterioration and in human alpha-synucleinopathies. J Clin Invest 110:1429–1439. CrossRef Medline

Orimo S, Uchihara T, Nakamura A, Mori F, Kakita A, Wakabayashi K, Takahashi H (2008) Axonal alpha-synuclein aggregates herald centripetal degeneration of cardiac sympathetic nerve in Parkinson's disease. Brain 131:642–650. CrossRef Medline

Pan-Montojo F, Anichtchik O, Dening Y, Knels L, Pursche S, Jung R, Jackson S, Gille G, Spillantini MG, Reichmann H, Funk RH (2010) Progression of Parkinson's disease pathology is reproduced by intragastric administration of rotenone in mice. PLoS One 5:e8762. CrossRef Medline

Saito Y, Kawashima A, Ruberu NN, Fujiwara H, Koyama S, Sawabe M, Arai T, Nagura H, Yamanouchi H, Hasegawa M, Iwatsubo T, Murayama S (2003) Accumulation of phosphorylated alpha-synuclein in aging human brain. J Neuropathol Exp Neurol 62:644–654. Medline

Sakisaka T, Yamamoto Y, Mochida S, Nakamura M, Nishikawa K, Ishizaki H, Okamoto-Tanaka M, Miyoshi J, Fujiyoshi Y, Manabe T, Takai Y (2008) Dual inhibition of SNARE complex formation by tomosyn ensures controlled neurotransmitter release. J Cell Biol 183:323–337. CrossRef Medline

Schulz-Schaeffer WJ (2010) The synaptic pathology of alpha-synuclein aggregation in dementia with Lewy bodies, Parkinson's disease and Parkinson's disease dementia. Acta Neuropathol 120:131–143. CrossRef Medline

Scott DA, Tabarean I, Tang Y, Cartier A, Masliah E, Roy S (2010) A pathologic cascade leading to synaptic dysfunction in α-synuclein-induced neurodegeneration. J Neurosci 30:8083–8095. CrossRef Medline

Sharma M, Burré J, Südhof TC (2011) CSPalpha promotes SNARE-complex assembly by chaperoning SNAP-25 during synaptic activity. Nat Cell Biol 13:30–39. CrossRef Medline

Shimazaki Y, Nishiki T, Omori A, Sekiguchi M, Kamata Y, Kozaki S, Takahashi M (1996) Phosphorylation of 25-kDa synaptosome-associated protein. Possible involvement in protein kinase C-mediated regulation of neurotransmitter release. J Biol Chem 271:14548–14553. CrossRef Medline

Shoji-Kasai Y, Itakura M, Kataoka M, Yamamori S, Takahashi M (2002) Protein kinase C-mediated translocation of secretory vesicles to plasma membrane and enhancement of neurotransmitter release from PC12 cells. Eur J Neurosci 15:1390–1394. CrossRef Medline

Spillantini MG, Goedert M (2000) The alpha-synucleinopathies: Parkinson's disease, dementia with Lewy bodies, and multiple system atrophy. Ann N Y Acad Sci 920:16–27. Medline

Südhof TC (2004) The synaptic vesicle cycle. Annu Rev Neurosci 27:509–547. CrossRef Medline

Tabuchi K, Blundell J, Etherton MR, Hammer RE, Liu X, Powell CM, Südhof TC (2007) A Neuroligin-3 mutation implicated in autism increases inhibitory synaptic transmission in mice. Science 318:71–76. CrossRef Medline

Tapia-González S, Giráldez-Pérez RM, Cuartero MI, Casarejos MJ, Mena MÁ, Wang XF, Sánchez-Capelo A (2011) Dopamine and alpha-synuclein dysfunction in Smad3 null mice. Mol Neurodegener 6:72. CrossRef Medline

Tong J, Wong H, Guttman M, Ang LC, Forno LS, Shimadzu M, Rajput AH, Muenter MD, Kish SJ, Hornykiewicz O, Furukawa Y (2010) Brain alpha-synuclein accumulation in multiple system atrophy, Parkinson's disease and progressive supranuclear palsy: a comparative investigation. Brain 133:172–188. CrossRef Medline

Ubhi K, Low P, Masliah E (2011) Multiple system atrophy: a clinical and neuropathological perspective. Trends Neurosci 34:581–590. CrossRef Medline

Wickens JR, Arbuthnott GW (2005) Structural and functional interactions in the striatum at the receptor level. In: Dopamine, Handbook of Chemical Neuroanatomy, Vol 21 (Dunnett SB, Bentivoglio M, Björklund A, Hökfelt T, eds), pp 199–236. Amsterdam: Elsevier.

Yamamori S, Itakura M, Sugaya D, Katsumata O, Sakagami H, Takahashi M (2011) Differential expression of SNAP-25 family proteins in the mouse brain. J Comp Neurol 519:916–932. CrossRef Medline

Yasuda T, Hayakawa H, Nihira T, Ren YR, Nakata Y, Nagai M, Hattori N, Miyake K, Takada M, Shimada T, Mizuno Y, Mochizuki H (2011) Parkin-mediated protection of dopaminergic neurons in a chronic MPTP-minipump mouse model of Parkinson disease. J Neuropathol Exp Neurol 70:686–697. CrossRef Medline

Yasuda T, Nakata Y, Mochizuki H (2012) α-Synuclein and neuronal cell death. Mol Neurobiol. Advance online publication. Retrieved November 8, 2012. doi:10.1007/s12035-012-8327-0. CrossRef

Yoshida M (2007) Multiple system atrophy: α-synuclein and neuronal degeneration. Neuropathology 27:484–493. CrossRef Medline

Imaizumi *et al. Molecular Brain* 2012, **5**:35
http://www.molecularbrain.com/content/5/1/35

Molecular Brain

RESEARCH Open Access

Mitochondrial dysfunction associated with increased oxidative stress and α-synuclein accumulation in PARK2 iPSC-derived neurons and postmortem brain tissue

Yoichi Imaizumi[1], Yohei Okada[1,2], Wado Akamatsu[1], Masato Koike[3], Naoko Kuzumaki[1], Hideki Hayakawa[4], Tomoko Nihira[4], Tetsuro Kobayashi[5], Manabu Ohyama[5], Shigeto Sato[6], Masashi Takanashi[6], Manabu Funayama[6,7], Akiyoshi Hirayama[8], Tomoyoshi Soga[8], Takako Hishiki[9], Makoto Suematsu[9], Takuya Yagi[10], Daisuke Ito[10], Arifumi Kosakai[10], Kozo Hayashi[11], Masanobu Shouji[11], Atsushi Nakanishi[11], Norihiro Suzuki[10], Yoshikuni Mizuno[12], Noboru Mizushima[13], Masayuki Amagai[5], Yasuo Uchiyama[3], Hideki Mochizuki[4,14], Nobutaka Hattori[6,7] and Hideyuki Okano[1*]

Abstract

Background: Parkinson's disease (PD) is a neurodegenerative disease characterized by selective degeneration of dopaminergic neurons in the substantia nigra (SN). The familial form of PD, PARK2, is caused by mutations in the *parkin* gene. *parkin*-knockout mouse models show some abnormalities, but they do not fully recapitulate the pathophysiology of human PARK2.

Results: Here, we generated induced pluripotent stem cells (iPSCs) from two PARK2 patients. PARK2 iPSC-derived neurons showed increased oxidative stress and enhanced activity of the nuclear factor erythroid 2-related factor 2 (Nrf2) pathway. iPSC-derived neurons, but not fibroblasts or iPSCs, exhibited abnormal mitochondrial morphology and impaired mitochondrial homeostasis. Although PARK2 patients rarely exhibit Lewy body (LB) formation with an accumulation of α-synuclein, α-synuclein accumulation was observed in the postmortem brain of one of the donor patients. This accumulation was also seen in the iPSC-derived neurons in the same patient.

Conclusions: Thus, pathogenic changes in the brain of a PARK2 patient were recapitulated using iPSC technology. These novel findings reveal mechanistic insights into the onset of PARK2 and identify novel targets for drug screening and potential modified therapies for PD.

Keywords: Induced pluripotent stem cells, Parkinson's disease, Parkin, Oxidative stress, Mitochondria, α-synuclein

Background

Parkin is a causative gene of autosomal recessive juvenile Parkinson's disease (PARK2). It encodes a component of an E3 ubiquitin ligase involved in mitochondrial homeostasis [1-5]. *Parkin* deficiency is thought to result in aberrant ubiquitination and compromised mitochondrial integrity, leading to neuronal dysfunction and degeneration. Several PARK2 mouse models exist, but they do not replicate all of the pathogenic changes seen in human PARK2 neurons; thus, these models do not fully account for the molecular mechanisms of PD [6-9]. A recent report demonstrated that there is a defect in dopamine (DA) utilization in PARK2 induced pluripotent stem cell (iPSC)-derived neurons [10]. However, it is not known whether neuronal homeostasis is disrupted in PARK2 patients. Furthermore, studies have yet to demonstrate whether the phenotype of PD-specific iPSC-derived neurons recapitulates the *in vivo* phenotype of the corresponding cell donor. To address these questions, we generated iPSCs from two PARK2 patients

* Correspondence: hidokano@a2.keio.jp
[1]Department of Physiology, Keio University School of Medicine, 35 Shinanomachi, Shinjuku-ku, Tokyo 160-8582, Japan
Full list of author information is available at the end of the article

BioMed Central

© 2012 Imaizumi et al.; licensee BioMed Central Ltd. This is an Open Access article distributed under the terms of the Creative Commons Attribution License (http://creativecommons.org/licenses/by/2.0), which permits unrestricted use, distribution, and reproduction in any medium, provided the original work is properly cited.

(PA and PB) [11]. In PARK2 iPSC-derived neurons, but not PARK2 fibroblasts or iPSCs, abnormal mitochondrial morphology and aberrant tubulovesicular structures adjacent to the Golgi were observed, as was increased oxidative stress. Although α-synuclein accumulation and Lewy body (LB) formation are very rare in PARK2 patients [1,12,13], we observed pathological changes and prominent LB formation, including the accumulation of α-synuclein, in postmortem brain tissue from one of the donor patients (PA). However, we obtained autopsied brain tissue from the father of donor PB, who carried the same *parkin* deletion as PB, and observed no evidence of LB formation or α-synuclein-positive cells. Consistent with these observations in postmortem brain tissue, increased α-synuclein accumulation was clearly observed in PA iPSC-derived neurons *in vitro,* but not in PB iPCS-derived neurons. These results are the first demonstration of pathogenic changes in the brain of a PARK2 patient that were recapitulated using iPSC technology. Our findings also provide mechanistic insights into PARK2 pathophysiology.

Results & discussion

Generation of PARK2 iPSCs

iPSCs were generated from dermal fibroblasts isolated from two PARK2 patients carrying *parkin* mutations and two control subjects using retroviruses carrying *Oct4, Sox2, Klf4,* and *c-Myc* to reprogram the cells as previously described [14,15]. The PARK2 patients were a 71-year-old female (PA) with a homozygous deletion of *parkin* exons 2–4 and a 50-year-old male (PB) with a homozygous deletion of exons 6 and 7 (Table 1 and Additional file 1A and B). Patient PA died 1 year after enrollment in the study at the age of 72. A previously-established human iPSC clone from control subject A, 201B7 (B7), was also used [15]. In addition, the following human embryonic stem cell (hESC)-like iPSC clones were selected for detailed analysis: three controls (B7 and YA9 from control A, and WD39 from control B), three from patient PA (PA1, PA9 and PA22), and four from patient PB (PB1, PB2, PB18 and PB20) (Figure 1A and Additional file 2A and B).

The PARK2 iPSCs expressed pluripotent hESC markers (Figure 1A and Additional file 2A-C) and formed teratomas containing all three germ layers (Additional file 2D).

Table 1 PA and PB patient information

	PA patient	PB patient
Race	Japanese	Japanese
Age	72 y/o	50 y/o
Sex	Female	Male
Age of onset	62 y/o	28 y/o
Mutation of *parkin*	Exon 2–4 homozygous deletions	Exon 6, 7 homozygous deletions

All of the retroviral transgenes were silenced in each clone (Additional file 2E). The iPSCs derived from PA and PB retained the corresponding homozygous *parkin* deletions and exhibited genomic stability (Figure 1B-D; Additional file 3A and B; and Table 1). All of the clones differentiated into neurons, including tyrosine hydroxylase (TH)-positive neurons, through a process of embryoid body and neurosphere formation (Figure 1A). Thus, all of the lines were successfully reprogrammed into a pluripotent state and were suitable for further analysis.

Increased oxidative stress accompanied by activation of the Nrf2 pathway in PARK2 iPSC-derived neurons

Because increased levels of oxidative stress have been documented in other PD models [7,10,16,17], we examined oxidative metabolism in the iPSC clones by measuring the cellular levels of reduced glutathione (GSH). GSH reacts with reactive oxygen species (ROS) and is catalyzed by glutathione S-transferase[18]. Consistent with previous results from patient-derived cells [16], the levels of GSH in PARK2 iPSC-derived neurospheres were significantly lower than those in control iPSC-derived neurospheres (Figure 2A). We also examined ROS production using 2', 7'-dichlorodihydrofluorescin (DCF) fluorescence to measure the levels of intracellular oxidants. The DCF fluorescence intensity in the PARK2 iPSC-derived neurons was significantly higher than that in control iPSC-derived neurons (Figure 2B and C), which indicated an increased level of oxidative stress. A recent study showed that, in PARK2 iPSC-derived neurons, monoamine oxidase (MAO)-A and -B levels and oxidative stress levels are increased, as is spontaneous DA release [10]. Here, we found no significant differences in MAO-A and -B expression levels between PARK2 and control neurons (Additional file 4A and B).

The Nrf2 pathway plays a cytoprotective role under conditions of ROS accumulation. Recent studies show that activation of the Nrf2 pathway reduces oxidative stress and provides partial protection from MPTP-mediated neurotoxicity[19]. Elevated Nrf2 expression was observed in the postmortem brain of a PD patient [20]. These data suggest a putative link between the Nrf2 pathway and PD, and prompted a closer investigation of this signaling pathway in control and PARK2 iPSC-derived neurons [19-21]. The expression of Nrf2 pathway proteins, such as Nrf2 and NADH quinone oxidoreductase (NQO1), was significantly increased in PARK2 iPSC-derived neurons (Figure 2D and E). These data are in line with previous reports [19-21], and suggest that the Nrf2 cytoprotective pathway may be activated in PARK2 iPSC-derived neurons to prevent further damage from oxidative stress. Taken together, these data demonstrated an increased level of

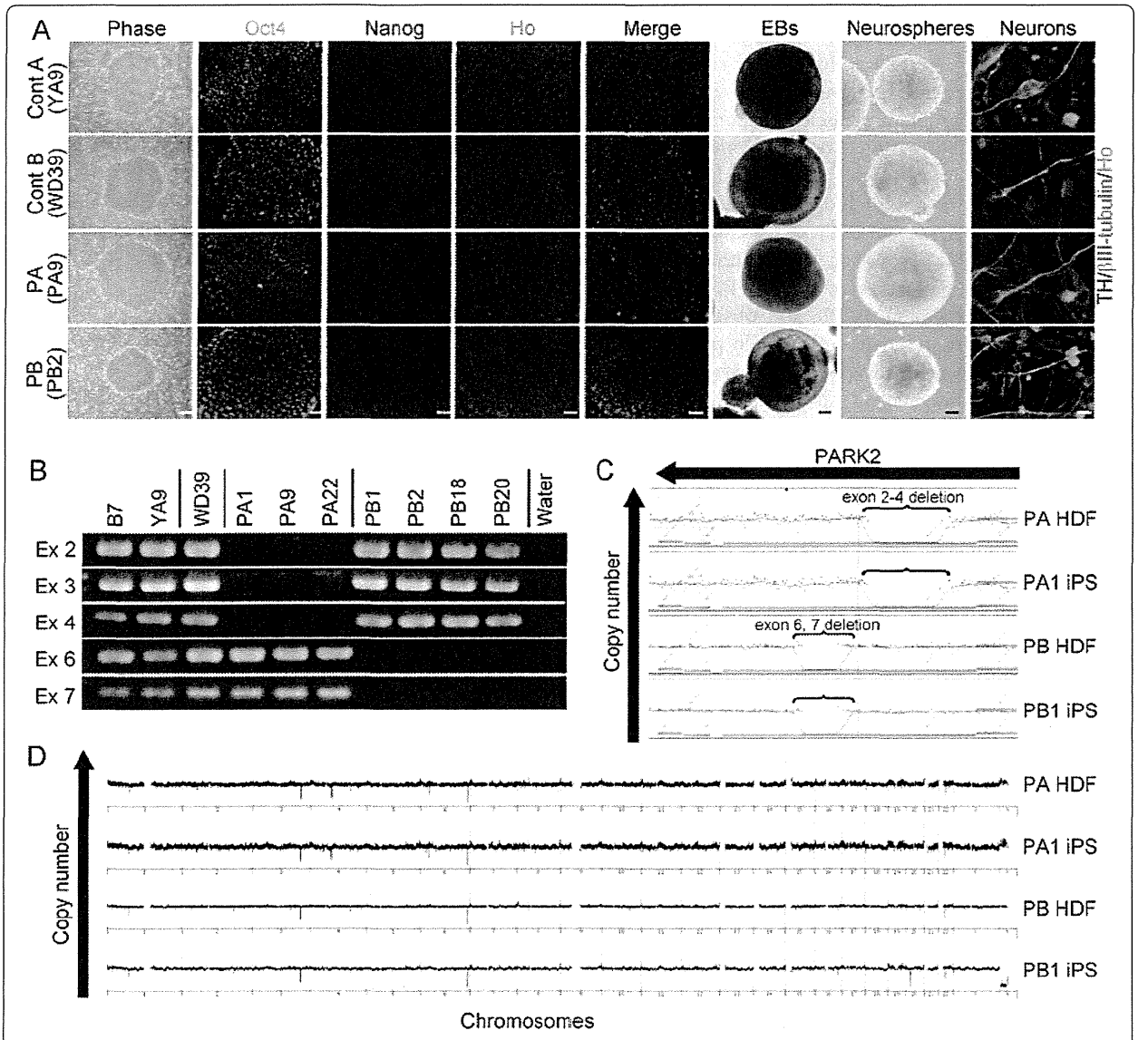

Figure 1 Generation of PARK2 iPSCs. (**A**) iPSCs derived from control and PARK2 subjects, embryoid bodies (EBs), neurospheres (NSs), and neurons. *Left three rows:* iPSCs from Control A (YA9), Control B (WD39), PA (PA9), and PB (PB2) were immunopositive for the pluripotency markers Oct4 (green) and Nanog (red). *Right three rows:* Differentiation of iPSCs into tyrosine hydroxylase (TH)-positive (red) neurons via EB and NS formation. Scale bars: Phase contrast, 400 μm; Nanog and Oct4 immunostaining, 100 μm; EBs, 25 μm; NSs, 50 μm; neurons, 10 μm. (**B**) Deletion of exons 2–4 in clones PA1, 9 and 22; and of exons 6 and 7 in clones PB1, 2, 18, and 20 was confirmed. (**C**) Exons 2–4 were deleted in human dermal fibroblasts (HDFs) from PA and in PA1 iPSC lines. Exons 6 and 7 were deleted in HDFs from PB and PB1 iPSC lines. (**D**) Copy number profiles of whole chromosomes in PARK2 HDFs and iPSCs were assessed by comparative genomic hybridization (CGH) microarray analysis; there was no evidence that genomic aberrations were introduced during the process of establishing PARK2 iPSCs.

oxidative stress accompanied by activation of the Nrf2 pathway in PARK2 neurons.

Abnormal mitochondrial morphology and impaired mitochondrial turnover in PARK2 iPSC-derived neurons

Increased oxidative stress (which affects anti-oxidant defense systems) and mitochondrial dysfunction are implicated in the pathogenesis of PD [1,13,21-23]. Furthermore, ROS accumulation causes both oxidative damage and mitochondrial dysfunction in the substantia nigra (SN) of *parkin*-deficient mice [7]. However, the exact mechanism of mitochondrial pathogenesis associated with PARK2 is controversial. For example, while *Drosophila parkin* mutants show abnormal mitochondrial morphology, *parkin*-knockout mice do not [7,24]. In addition, while a greater degree of mitochondrial branching is observed in

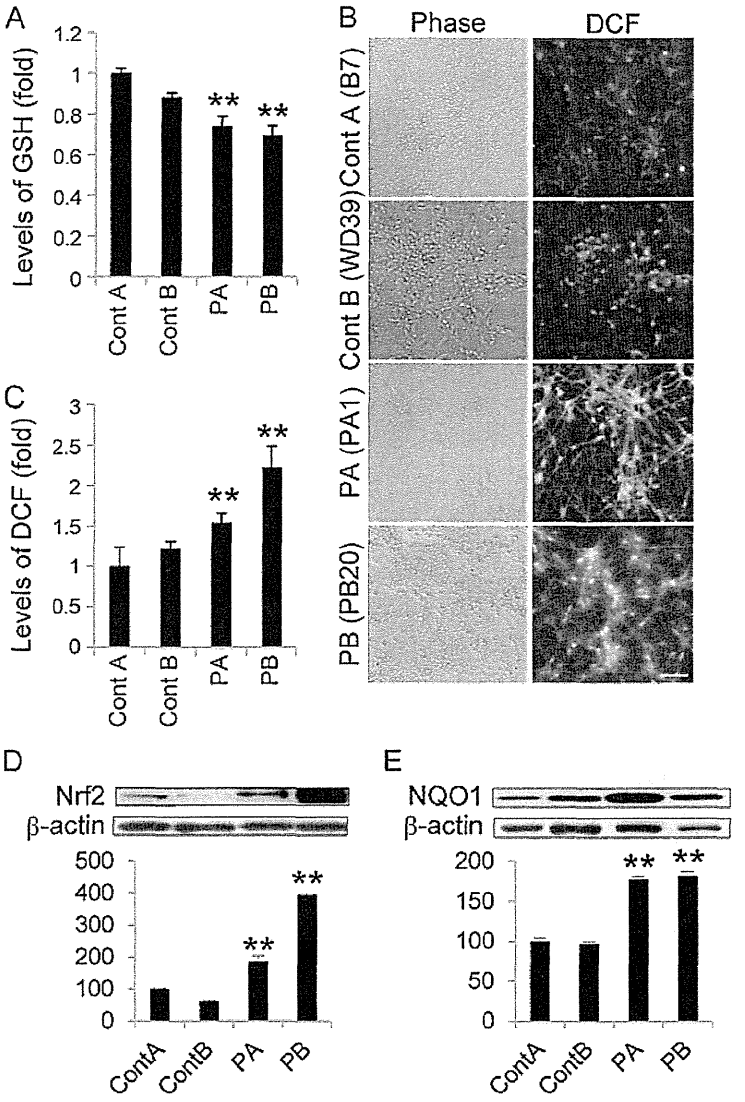

Figure 2 Increased oxidative stress accompanied by activation of the Nrf2 pathway in PARK2 iPSC-derived neurons. (**A**) GSH levels were significantly reduced in PARK2 (PA1, 9 and 22, and PB2, 18 and 20) iPSC-derived neurospheres compared with those in control A (YA9) and B (WD39) neurospheres. (**B, C**) DCF fluorescence intensity in PARK2 (PA1, 9 and 22, and PB2 and 20) iPSC-derived neurons was significantly higher than that in control A (B7) and B (WD39) neurons. (**D, E**) Immunoblot analysis of Nrf2 and NQO1 levels in iPSC-derived neurons from PA and PB. Expression of Nrf2 and NQO1 in PARK2 (PA9 and PB2) iPSC-derived neurons was significantly higher than that in control A (YA9) and B (WD39) neurons. Relative protein abundance was normalized to β-actin. ** indicates $P < 0.01$ (Mann–Whitney *U*-test). Data represent the mean and SEM of at least three experiments for each group.

fibroblasts derived from PARK2 patients, the detailed morphology of the mitochondria in these cells has not been characterized [25]. To investigate these mitochondrial abnormalities in more depth, we performed a detailed morphological analysis of mitochondria in PARK2 iPSC-derived neurons using electron microscopy. Mitochondria in PARK2 neurons from both patients showed a highly electron-dense matrix and swollen mitochondrial cristae within the inner mitochondrial membrane (IMM) (Figure 3A, black arrowheads). The perikaryal volume density of the abnormal mitochondria was significantly increased in PA and PB iPSC-derived neurons relative to control clones (Figure 3B). Furthermore, the density of normal mitochondria decreased (Figure 3B). Importantly, both abnormal and normal mitochondria were observed in PARK2 neurons (Figure 3A, white arrowheads). Abnormal mitochondria were observed in 87.8% of iPSC-derived neurons from PA, and 79.5% of iPSC-derived neurons from PB. These data indicated that abnormal mitochondrial morphology was a feature of most PARK2 iPSC-derived

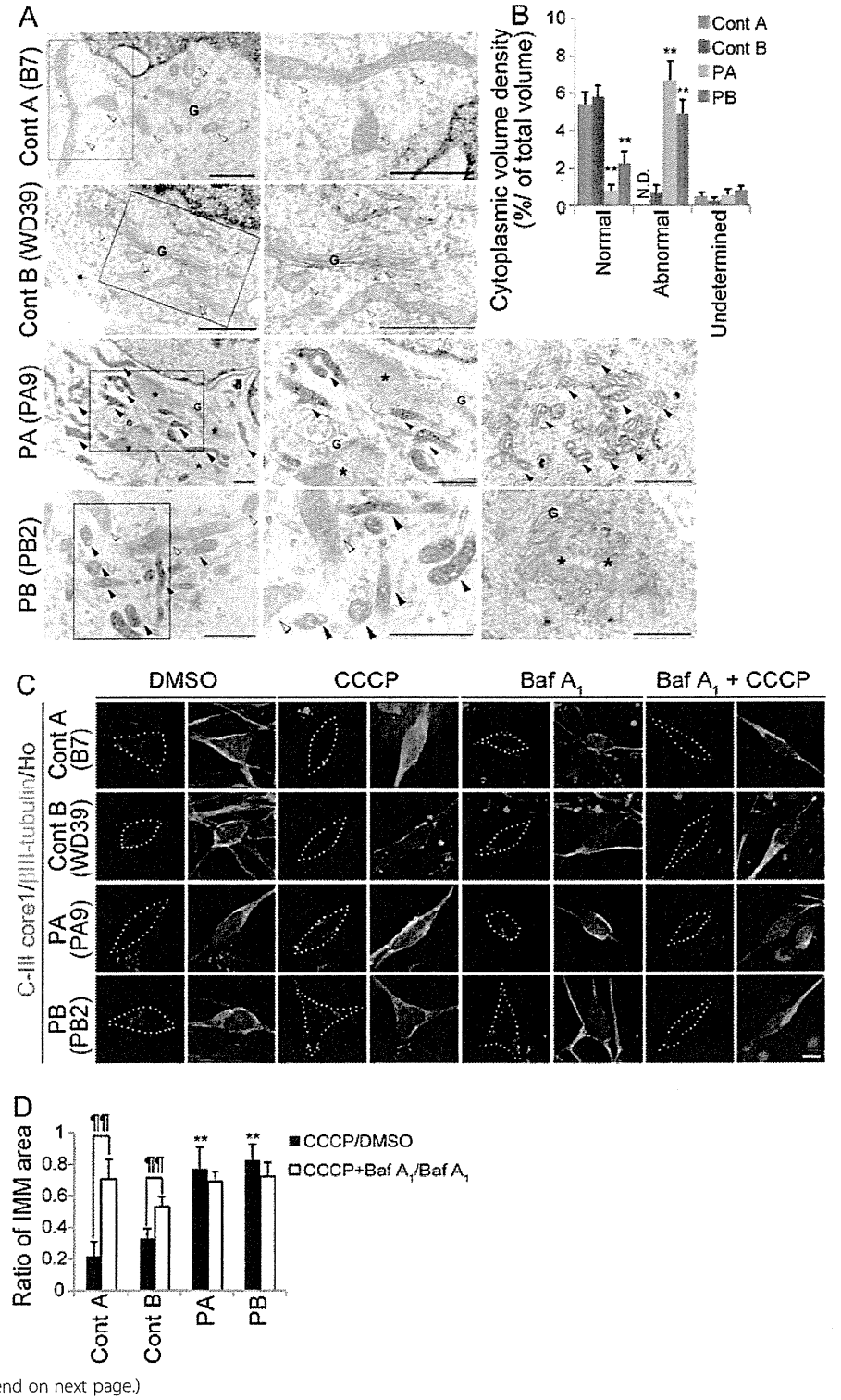

Figure 3 (See legend on next page.)

(See figure on previous page.)
Figure 3 Dysregulation of mitochondrial homeostasis in PARK2 iPSC-derived neurons. (**A**) Electron micrographs of control A (B7), control B (WD39) and PARK2 (PA9 and PB2) iPSC-derived neurons. Boxed areas are shown in the enlarged images to the right. Control mitochondria showed a characteristically long, cylindrical profile with well-organized cristae, and the electron density of the matrix was relatively low (white arrowheads). By contrast, increased electron density of the matrix was evident in PARK2 mitochondria (black arrowheads), and the cristae often appeared swollen. As shown in PB2, some of the neurons contained both morphologically intact (white arrowheads) and abnormal (black arrowheads) mitochondria. Furthermore, abnormal tubulovesicular structures (asterisks) were observed adjacent to the Golgi cisternae (G). (**B**) The relative perikaryal volume of the abnormal mitochondria was significantly increased, and that of the normal mitochondria was decreased, in PARK2 neurons compared with control neurons. (**C**) Double labeling for the IMM marker, ComplexIII corel (CIII-Core I; magenta) and βIII-tubulin (green) of control A (B7), control B (WD39) and PARK2 (PA9 and PB2) iPSC-derived neurons. The volume of the IMM area was reduced in control neurons treated with CCCP, but not in PARK2 neurons treated with CCCP. Administration of Baf A_1 rescued the CCCP-induced phenotype in control neurons. (**D**) The CCCP/DMSO ratio in control A (B7 and YA9) and B (WD39) neurons was reduced after CCCP treatment. This reduction was not observed in PARK2 (PA1, 9 and 22, and PB2 and 20) iPSC-derived neurons (black bars indicate CCCP/DMSO ratio; white bars indicate Baf A_1+CCCP/Baf A_1 ratio). ** indicates $P < 0.01$ compared with the control; ¶¶ indicates $P < 0.01$ when comparing the black and white bars (Mann–Whitney *U*-test). At least three experiments were performed for each group, with 5–36 cells quantified per experiment. Scale bars: a, 1 μm; c, 10 μm. Error bars represent the SEM. N.D., not detected.

neurons from these patients. In addition, abnormal tubulovesicular structures were observed adjacent to the Golgi cisternae in PARK2 iPSC-derived neurons (Figure 3A). These abnormal mitochondrial and tubulovesicular structures were not observed in PARK2 fibroblasts or in undifferentiated iPSCs (Additional file 5A and B). These histological abnormalities represent novel PARK2-related neuronal pathologies.

PARKIN is involved in the mitochondrial fission/fusion system and is recruited to depolarized mitochondria to promote mitophagy [5,26-29]. In iPSC-derived neurons containing a mutation in PINK1 (a protein kinase upstream of PARKIN), PARKIN is not recruited appropriately to mitochondria [30]. We hypothesized that PARKIN-deficient human neurons would show aberrant removal of depolarized mitochondria. To examine the turnover of damaged mitochondria, we treated iPSC-derived neurons with carbonyl cyanide m-chlorophenyl hydrazine (CCCP), which triggers the loss of mitochondrial membrane potential and results in the removal of damaged mitochondria. The intensity of TMRE, a mitochondrial membrane potential-dependent dye, clearly decreased in both control and PARK2 iPSC-derived neurons treated with CCCP, which indicated a reduced mitochondrial membrane potential in both sets of neurons (Additional file 6). To determine the extent to which the damaged mitochondria were eliminated, we measured the area of the IMM after CCCP treatment. Compared with untreated cells, there was a dramatic loss of IMM area in the treated control neurons, but not in the treated PARK2 neurons (Figure 3C, left four columns; Figure 3D, black bars). To assess whether lysosomes were involved in the CCCP-induced elimination of mitochondria, we treated cells with Bafilomycin (Baf) A_1, an inhibitor of the vacuolar type H(+)-ATPase. Baf A_1 attenuated the CCCP-dependent reduction in the IMM area in control neurons (Figure 3C, right four columns; Figure 3D, white bars). To confirm that the abnormal turnover of damaged mitochondria was characteristic of neuronal cells, PARK2 fibroblasts and undifferentiated iPSCs were treated with CCCP. CCCP-treated PARK2 fibroblasts and undifferentiated iPSCs exhibited the same mitochondrial dynamics as CCCP-treated control cells (Additional file 5C-E). Together, these data indicated aberrant degradation of mitochondria damaged by CCCP treatment in PARK2 iPSC-derived neurons.

These results support a recently proposed working model for PD, in which damaged mitochondria accumulate due to a disruption in PARKIN-mediated mitochondrial quality control [28]. The electron microscopy data, which showed a mixture of abnormal and normal mitochondria, indicated that PARKIN-mediated mitochondrial quality control is compromised, even in young PARK2 iPSC-derived neurons. In these cells, residual normal mitochondria may have compensated for the damaged ones. Thus, while our findings suggest that the PARKIN-dependent mechanisms that regulate mitochondrial homeostasis are disrupted in PARK2 cells, further detailed analyses are required to fully understand the mechanism underlying this disruption and the implications for PD.

Patient-specific accumulation of α-synuclein in PARK2 iPSC-derived neurons and its correlation with LB formation

LBs are pathological neuronal inclusions composed principally of α-synuclein. They are typically associated with PD and certain forms of dementia [1,13,31]. Although LBs are generally thought to be absent from PARK2 patients [1,13,31], rare cases of LB formation in the brains of PARK2 patients have been reported recently [12,32,33]. The PARKIN protein co-localizes with LBs in some patients with sporadic PD [34], and a functional interaction between PARKIN and α-synuclein is indicated by both *in vitro* and *in vivo* findings [35-37]. These results suggest that PARKIN-pathway may contribute to LB formation in PD patients.

We were able to conduct a histopathological analysis of postmortem brain tissue from patient PA. Hematoxylin and eosin staining of the SN revealed low levels of brown-black

melanin pigment compared with healthy SN tissue (Figure 4A and A'). Surprisingly, LBs accumulated in the SN and other areas of the brain in patient PA (Figure 4B and Table 2). Furthermore, α-synuclein and pα-synuclein immunoreactive puncta and neurites were observed in the areas where LBs were present (Figure 4B). TH/pα-synuclein double-positive neurons were also detected in the SN (Figure 4C). Of note, α-synuclein-positive/TH-negative or pα-synuclein-positive/TH-negative neurons in the SN and other areas of the brain tissue from patient PA's brain were observed (Table 2). These data suggested that α-synuclein accumulated not only in TH+ neurons, but also in other types of neurons. Postmortem tissue from the brain of the father of patient PB was also examined. The father carried a homozygous deletion of exons 6 and 7 of the *parkin* gene (Figure 1B, Additional file 1B and 7A), similar to patient PB. There was no evidence of LBs or α-synuclein-positive neurons in the autopsied brain tissue of the father (Figure 4D). Thus, since the genetic background of patient PB and his father are likely to be very close (Additional file 1B and 7A), these results are probably reflective of a specific phenotype of patient PB, which was different from that in patient PA (Figure 4A-D).

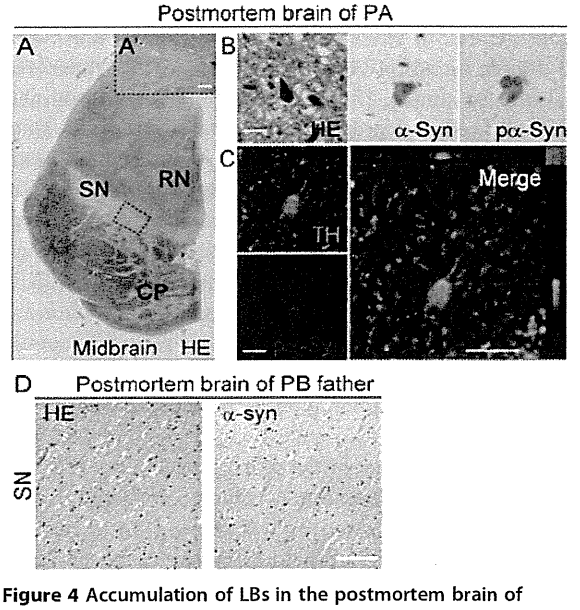

Figure 4 Accumulation of LBs in the postmortem brain of patient PA. (**A**–**C**) Immunohistochemical staining of postmortem brain tissue from patient PA. (**A**) Low magnification image of a midbrain section stained with hematoxylin and eosin (H&E). (**A'**) High magnification image of the boxed area. Melanin levels were reduced in most of the substantia nigra (SN). (**B**) (Left) High magnification image of a midbrain section stained with H&E showing the presence of Lewy bodies (LBs) in the SN. (Middle and Right) α-synuclein-positive and pα-synuclein-positive cells in the SN. (**C**) Confocal microscopy image of a TH (green) and pα-synuclein (red) double-positive SN neuron and a projected merged image: pα-synuclein accumulated in the TH-positive neuron. (**D**) Melanin levels were reduced in most of the SN. No LBs or α-synuclein-positive neurons were observed in postmortem brain tissue from the father of patient PB. Scale bars: A, 1000 μm; A', 350 μm; B, C, 50 μm; D, 100 μm.

To determine whether iPSC-derived neurons recapitulated the *in vivo* phenotypes of the corresponding cell donors, we next examined α-synuclein accumulation in PARK2 iPSC-derived neurons. To rule out the possibility that α-synuclein expression in undifferentiated PARK2 iPSCs was increased by multiplication of the *SNCA* gene, genomic aberrations acquired during the process of iPSC establishment, or by repeated passage of the cells, the *SNCA* gene copy number in iPSCs was quantified by genomic qPCR. A comparison with control iPSCs showed that iPSCs from both PA and PB carried the normal number of *SNCA* gene copies (Additional file 8A). Moreover, immunostaining for α-synuclein did not reveal any increase or decrease in α-synuclein protein levels in PARK2 iPSCs (Additional file 8B). As a control for LB formation, we generated iPSC-derived neurons from a 106-year-old woman (designated Cent1-8), since previous work suggested that aging is a predisposing factor for LB formation in PD patients [31,38]. Since α-synuclein was also expressed in non-neural cells, triple labeling for α-synuclein, βIII-tubulin, and TH was performed to ensure that only neurons were examined (Figure 5A, asterisks). The proportion of α-synuclein-positive iPSC-derived neurons that were also positive for βIII-tubulin from PB was similar to that in the controls (including Cent1-8); however, the proportion was significantly higher in PA. These results were consistent with the *in vivo* phenotypes of the cell donors based on analysis of postmortem brain tissue (1629, 357, 805, 3747, and 4330 iPSC-derived βIII-tubulin+ neurons in control A, control B, Cent1-8, PA and PB respectively; Figure 5A-C, arrows and arrowheads). Thus, the increase in α-synuclein expression levels seen in PARK2 iPSC-derived neurons

Table 2 LB type pathology in PA patient's postmortem brain

Brain area		LB type pathology
Brainstem lesion	IX-X	+++
	LC	+++
	SN	++
Basal forebrain/Limbic	nbM	++
	Amy	++
	Ent	+
	Cing	+
Neocortical	T	-
	F	-
	P	-

IX-X, motor cranial nerves IX-X; *LC*, Locus Coeruleus; *SN*, Substantia Nigra; *nbM*, nucleus basal of Meynert; Amy, Amygdala; Ent, Entorhinal cortex; T, Temporal lobe; F, Frontal lobe; P, Parietal lobe.

cannot be attributed solely to the effects of aging, but associated with the disease phenotype.

The obvious LB-formation was observed in the postmortem brain of PA patient, who showed a late onset at 61 years, corresponding to the enhanced α-synuclein accumulation in the iPSC-derived neurons from the same patient. Thus, it is likely that early-stage LB formation was recapitulated *in vitro* in iPSC-derived neurons. Furthermore, the present findings are consistent with recent work by several groups, which suggest that the age of onset of PARK2 in patients with LB formation (41 on average) is later than in patients without LB formation (below 40) [12,32,33]. The earlier onset in patient PB (at 28 years) than in PA (at 61 years) would be consistent with the finding of lower α-synuclein accumulation in PB iPSC-derived neurons compared with PA iPSC-derived neurons. On the other hand, and in contrast to the observations of brain tissue from PA, analysis of brain tissue from the father of patient PB, in whom the onset of PD was 39 years of age, revealed no evidence of LB formation (Figure 4D). Importantly, PA iPSC-derived neurons showed significantly more α-synuclein accumulation than PB iPSC-derived neurons (Figure 5A and C). These results suggest that the extent of α-synuclein accumulation is an important factor in LB formation. Then, how can we explain the difference of α-synuclein accumulation between PA and PB patients-derived neuronal cells? It is possible that PA is a rare example of PARK2 complicated by sporadic PD. Although both PA and PB iPSCs showed a normal *SNCA* gene copy number, it is possible that PA-derived cells acquired an unknown gene mutation relating to LB formation. Thus, we cannot rule out the possibility that other factors may affect LB formation in PARK2 patients. Further analyses will be required to identify these putative factors. Although iPSC clones from sporadic and familial PD patients were recently established [17,30,39-42], this report is the first to demonstrate that the phenotype of PD-specific iPSC-derived neurons replicates the *in vivo* phenotype seen in postmortem brain tissue from the corresponding cell donor.

Conclusions

In summary, dysfunctional neuronal homeostasis (characterized by increased oxidative stress and activation of the Nrf2 pathway), impaired mitochondrial function, and increased α-synuclein accumulation were observed in PARK2 iPSC-derived neurons. These results indicate that PARK2-associated phenotypes may appear soon after, or possibly even before, the onset of PARK2. Detailed analyses of PARK2 iPSC-derived neurons, particularly mature neurons, to determine the time course of LB accumulation and synaptic dysfunction will be of great interest. Such analyses will further our understanding of the pathogenesis of PARK2 as well as sporadic PD. The ultimate goal is the development and application of novel preventative therapies for PD.

Materials & methods

Isolation of human skin fibroblasts and generation of iPSCs

For control A, human dermal fibroblasts (HDFs) from the facial dermis of a 36-year-old Caucasian female (Cell Applications Inc.) were used to establish iPSCs (201B7; Passage 20–29, YA9; Passage 15–24). The 201B7 iPSCs were kindly provided by Dr. Yamanaka [15]. A skin-punch biopsy from a healthy 16-year-old Japanese female obtained after written informed consent (Keio University School of Medicine) was used to generate the control B iPSCs (WD39; Passage 8–17). PA iPSCs (PA1, 9, and 22; Passage 10–19) and PB iPSCs (PB1, 2, 18, and 20; Passage 8–17) were generated from a 71-year-old Japanese female patient and a 50-year-old Japanese male patient, respectively, using the same methods used to generate control B iPSCs. The maintenance of HDFs, lentiviral production, retroviral production, infection, stem cell culture and characterization, and teratoma formation were performed as described previously [14,15]. All of the experimental procedures for skin biopsy and iPS production were approved by the Keio University School of Medicine Ethics committee (Approval Number: 20-16-18) and Juntendo University School of Medicine Ethics committee (Approval Number: 2012068). hESCs (KhES-1; Passage 29–38 (kindly provided by Dr. Norio Nakatsuji) were cultured on feeder cells in iPS culture media [43].

In vitro differentiation of human iPSCs

Neural differentiation of iPSCs was performed as previously described [44] with slight modifications (Okada et al., manuscript in preparation). Briefly, iPSC colonies were detached from feeder layers and cultured in suspension as EBs for about 30 days in bacteriological dishes. EBs were then enzymatically dissociated into single cells and the dissociated cells cultured in suspension in serum-free media (MHM) [44] for 10 to 14 days to allow the formation of neurospheres. Neurospheres were passaged repeatedly by dissociation into single cells followed by culture in the same manner. Typically, neurospheres between passages 3 and 8 were used for analysis. For terminal differentiation, dissociated or undissociated neurospheres were allowed to adhere to poly-L-ornithine- and fibronectin-coated coverslips and cultured for 10 days.

Immunocytochemical analysis of iPSCs and neurons

For immunocytochemical analysis, cells were fixed with phosphate buffered saline (PBS) containing 4% paraformaldehyde (PFA) for 30 min at room temperature (RT). The cells were analyzed by immunofluorescence staining using antibodies to the following proteins: β-III-tubulin (1:1000,

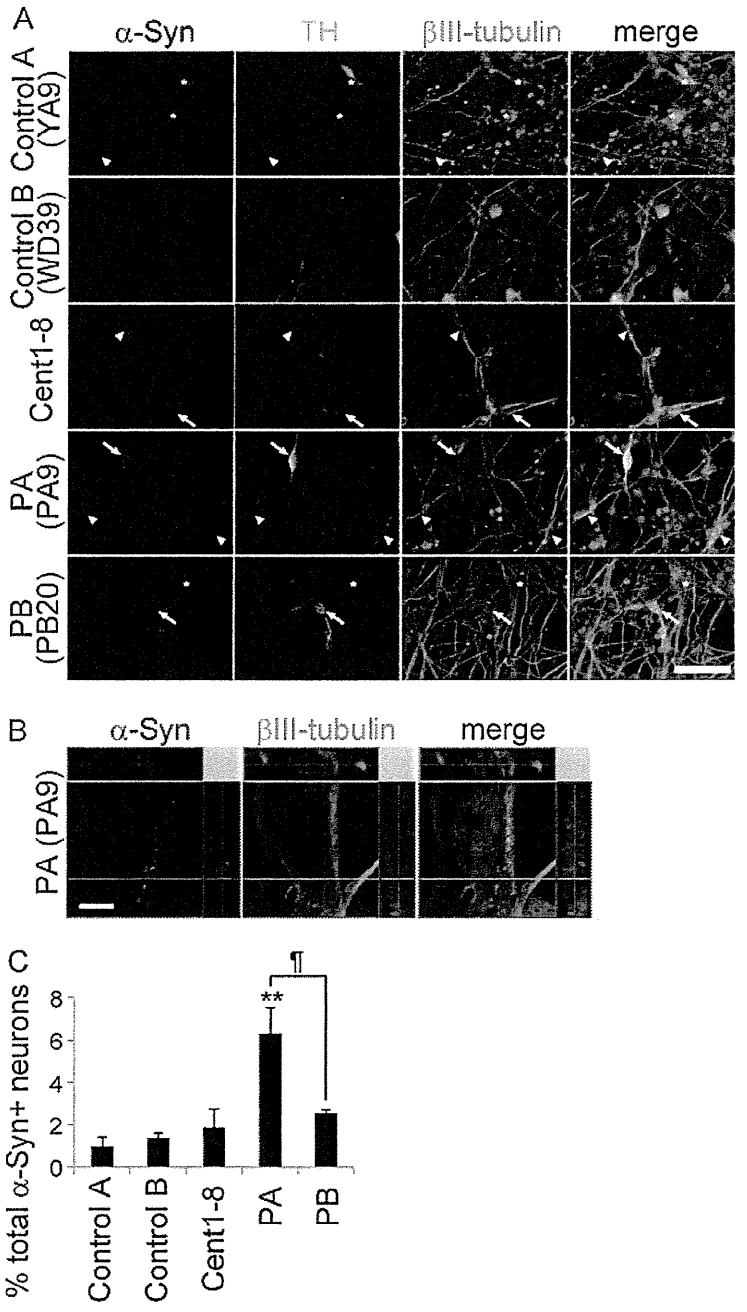

Figure 5 α-synuclein accumulation in PARK2 iPSC-derived neurons. (**A**–**C**) Triple labeling for α-synuclein (red), tyrosine hydroxylase (TH; cyan), and βIII-tubulin (green) along with Hoechst (blue) staining of control A (B7), control B (WD39), Cent1-8, and PARK2 (PA9 and PB20) iPSC-derived neurons. (**A**) Arrows indicate α-synuclein+/TH+/βIII-tubulin+ neurons; arrowheads indicate α-synuclein+/TH-/βIII-tubulin+ neurons. Note the presence of α-synuclein+/TH-/βIII-tubulin- non-neural cells (asterisks). (**B**) High magnification confocal projection image of an α-synuclein (magenta)/βIII-tubulin (green) double-positive PA9 iPSC-derived neuron. (**C**) The proportion of α-synuclein+/βIII-tubulin+ neurons relative to βIII-tubulin-positive neurons was significantly higher in PA (PA1, 9 and 22) iPSC-derived neurons than in control A (B7 and YA9), control B (WD39) and Cent1-8 iPSC-derived neurons. Scale bars: A, 50 μm; C, 5 μm. ** indicates $P < 0.01$; * and ¶ indicate $P < 0.05$ (Mann–Whitney *U*-test). Data represent the mean and SEM of at least three experiments for each group.

Sigma), NANOG (1:100, ReproCELL), OCT3/4 (1:200, Santa Cruz Biotechnology), SSEA-4 (1:200, Millipore), TRA-1-60 (1:200, Millipore), TH (1:100, Millipore), α-synuclein (1:500, Invitrogen), pα-synuclein (1:1000, Wako), cleaved-Caspase3 (1:500, Cell Signaling) and ComplexIII (C-III)-core I (1:200, Invitrogen). Cells were washed with PBS after incubation with the primary antibody, followed by incubation with an Alexa Fluor 488-, Alexa Fluor 555-, or Alexa Fluor 647-conjugated secondary antibody (1:500, Invitrogen). Images were obtained using Apotome (Zeiss) or LSM-710 confocal (Zeiss) microscopes.

PCR amplification of genomic DNA

Genomic DNA was purified from HDFs and iPSCs using a DNeasy kit (Qiagen). The PCR conditions used have been previously described [2,42].

Reverse transcription (RT)-PCR

RNA isolation and reverse transcription (RT)-PCR were performed as previously described [44]. The amount of cDNA was normalized to *β-actin* mRNA. Real-time RT-PCR was performed on a ABI PRISM Sequence detection System 7900HT (Applied BioSystems) using SYBR premix ExTaq (Takara). Primers for the detection of Oct4, the transgenes *Oct4-tg, Sox2-tg, Klf4-tg* and *c-Myc-tg*, and MAO-A, and -B have been previously described [10,15].

Teratoma assay

To assess teratoma formation, iPSCs were injected into the testis of 8-week-old NOD/SCID mice (OYG International) as previously described [14]. Eight weeks after transplantation, tumors were dissected and fixed with 4% PFA in PBS. Paraffin-embedded tissue was sectioned and stained with H&E. Images were obtained using a BZ-9000 (Keyence) microscope.

CGH array

Genomic DNA was restricted, labeled, and purified using the Agilent Oligo CGH Microarray Kit (Agilent Technologies) according to the manufacturer's protocol. Labeled genomic DNA was processed for hybridization on a 4x 180K microarray (Agilent Technologies). Processing was performed as instructed by the manufacturer. The genomic analysis was performed using Agilent Genomic Workbench ver. 6.0 software (Agilent Technologies).

Metabolism assays

Reduced GSH levels were measured according to the kit manufacturer's protocol (GSH-Glo Glutathione Assay; Promega). Chymotrypsin-like proteasome activity was measured using a Cell-Based Proteasome-Glo Assay according to the manufacturer's instructions (Promega). Briefly, neural cells (1.0×10^4) derived from neurospheres were seeded in triplicate into a white 96-well plate (Nunc). Prepared reagent (100 μl) was added to each well. After incubation for 10 min at RT, luminescence intensity was recorded. ROS levels were determined by measuring DCFH-DA fluorescence (Invitrogen). Briefly, neurons were incubated with 5 μM DCFH-DA and Hoechst (1:2000) for 30 min at 37°C, after which they were washed with PBS and then incubated in differentiation media. Fluorescence was measured by an In Cell Analyzer 2000 system (GE Healthcare Biosciences).

Protein analysis

Differentiated neurons were harvested in MAPK lysis buffer containing proteinase inhibitor, and protein concentrations were measured by BCA assay (Thermo Scientific). Samples were diluted to yield equivalent protein concentrations and then 4 μg was denatured by the addition of 4X sample buffer (Invitrogen) supplemented with β-mercaptoethanol followed by boiling. Samples (7 μl/lane) were loaded onto a 4–20% SDS-polyacrylamide gradient gel. Membranes were incubated in blocking solution with the indicated primary antibodies at 4°C overnight. Immunoreactive proteins were detected with horseradish peroxidase (HRP)-conjugated secondary antibodies and then visualized by chemiluminescence (Pierce, Rockford, IL, USA) according to the manufacturer's instructions. Quantification of band intensities was performed using an RAS4000 system. The primary antibodies used were anti-NQO1 (1:1000, Abcam), anti-NRF2 (1:1000, Santa Cruz Biotechnology) and β-actin (1:5000, Cell Signaling).

CCCP and Baf A_1 treatments

Neurons were cultured with 30 μM CCCP (Sigma-Aldrich) or DMSO, with or without 5 μM Baf A_1 (Sigma-Aldrich), for 48 h. The cells were then fixed and stained for βIII-tubulin and C-III Core I, and counterstained with Hoechst. To quantify the IMM area of the neurons, the cytoplasmic area was extracted as shown in Figure 3C. The C-III Core I-positive signals within the extracted area were then converted to gray-scale and digitized. The IMM area was quantified from the digitized values using Image J software.

Tetramethylrhodamine ethyl ester (TMRE) staining

iPSC-derived neurons were incubated with 1nM TMRE (Invitrogen) for 15 min at 37°C and then observed under an Olympus IX81 microscope.

Electron microscopy

Cells were fixed with 2% glutaraldehyde/2% PFA in 0.1 M phosphate buffer (PB) (pH7.2), post-fixed with 1% OsO4 in 0.1 M PB (pH 7.2), blocked and stained with a 2% aqueous solution of uranyl acetate, dehydrated with a graded series of ethanol, and then embedded in Epon 812 (TAAB). Coverslips were detached and the embedded samples were placed under a stereomicroscope to identify the cells of

interest. Ultrathin sections were cut with a Leica UC6 or UC7 ultramicrotome (Leica Microsystems) and then stained with uranyl acetate and lead citrate. Samples were observed with a Hitachi H7100 or HT7700 electron microscope.

Morphometry

Morphometric analysis was used to measure the volume density of mitochondria in the neuronal perikarya as previously described [45]. Briefly, electron micrographs of neurons (n = 20, 23, 41, and 44 for control A (B7), control B (WD39), PA9 and PB2, respectively) were obtained at a magnification of ×7000. After enlarging to three times the original magnification, point-counting was carried out to determine the volume density using a double-lattice test system with 1.5 cm spacing. Mitochondria were classified as normal, abnormal, or undetermined. The abnormal mitochondria were defined as those with irregularly arranged cristae, or with a high electron-dense matrix. The volume density (Vv) of each type of mitochondrion was expressed as percent volume according to the following formula: Vv = (Pi/Pt) × 100 (%), where Pi is the number of points falling on each mitochondrial structure and Pt is the number of points falling on the neuronal perikarya.

Immunohistochemical analysis of autopsied brain tissue

The ethical committee of the Kitasato University School of Medicine and Juntendo University School of Medicine reviewed and approved the protocol for analysis of autopsied brain tissue. Patients and control subjects were informed of the study and gave written informed consent. Brain tissue from patient PA was obtained following her death at age 72; brain tissue from the father of patient PB was obtained when he died at age 70 [46]. Tissue was fixed with 10% formalin and then embedded in paraffin. Midbrain sections (6 μm thick) were cut, deparaffinized with xylene, and then rehydrated in ethanol. After being boiled and treated with H_2O_2, sections were subjected to immunofluorescence staining with antibodies to the following proteins: α-synuclein (1:500, Invitrogen), pα-synuclein (1:1000, Wako), and TH (1:1000, Calbiochem). After washing with PBS, sections were incubated with a biotinylated secondary antibody (1:500; Vector Laboratories Inc.) at RT for 1 hr followed by incubation with an avidin-biotin peroxidase complex (Vector Laboratories Inc.) for 1 hr. Immunoreactive proteins were visualized using 3,3-diaminobenzidine (DAB; Wako Pure Chemical Industries) and nuclear fast red staining. For immunofluorescence, FITC-conjugated and Cy3-conjugated secondary antibodies (1:500; Jackson Immunoresearch Laboratories) were used. Images were obtained using a BIOREVO (Keyence) and a confocal laser-scanning LSM710 (Zeiss) microscope.

Statistical analysis

Values represent the mean ± SEM. The Mann–Whitney *U*-test was used to evaluate differences between groups. A P value of < 0.05 was considered significant.

Additional files

Additional file 1: Genetic studies of family. (A) An arrow indicates PA patient. (B) An arrow indicates PB patient. Filled circles and squares, women and men with PARK2 mutation; Open circles and squares, normal women and men; Diamond shapes, family members whose DNA samples were not analyzed. Symbols with lines through them represent the deceased.

Additional file 2: Characterization of control and PARK2 iPSCs. (A) Control A (YA9), Control B (WD39), PA (PA9), and PB (PB2) iPSCs expressed the pluripotency markers SSEA4 (red) and TRA1-60 (green). Scale bar, 100 μm. (B) iPSCs established from patients PA (PA1, PA22) and PB (PB1, PB18, and PB20) were positive for the pluripotency markers Nanog (red), Oct4 (green), SSEA4 (red), and TRA1-60 (green). Scale bars: phase images, 200 μm; immunofluorescence images, 100 μm. (C) Levels of endogenous *Oct4* mRNA in the generated iPSCs were similar to those in KhES1 cells, a human embryonic stem cell (hESC) line [42]. Expression levels were normalized to that of KhES1 (set as 1). (D) Cont A (YA9), Cont B (WD39), PA (PA1, 9 and 22), and PB (PB1, 2, 18 and 20) iPSCs gave rise to teratomas with all three germ layers, confirming pluripotency. Scale bar, 100 μm. (E) Silencing of transgenes in control and PARK2 iPSC clones. Expression levels were normalized to the positive control of fibroblasts in cultures assayed 6 days after retroviral infection (= 100). Cont A, Control A; Cont B, Control B.

Additional file 3: Confirmation of *parkin* deletions and genomic stability of PARK2 iPSCs using comparative genomic hybridization (CGH) microarray analysis. (A) Exons 2–4 were deleted in the PA9 and PA22 iPSC lines. Exons 6 and 7 were deleted in the PB2, 18, and 20 iPSC lines. (B) Copy number profiles of whole chromosomes in PARK2 iPSCs assessed by CGH microarray analysis revealed that no genomic aberrations were introduced during the process of establishing PARK2 iPSCs.

Additional file 4: Expression level of MAO-A and -B showed no difference among Control and PARK2 iPSC-derived neurons. (A,B) qRT-PCR measurement of MAO-A and -B transcripts in PARK2 (PA (1, 9 and 22) and PB (1, 2 and 20)) iPSC-derived neurons showed no difference compared to those in Cont A (B7 and YA9). ContA; Control A, ContB; Control B.

Additional file 5: Healthy mitochondria in PARK2 fibroblasts and iPSCs. (A, B) Electron micrographs of fibroblasts (upper panels) and iPSCs (lower panels) from Control (Cont A and Cont B) and PARK2 patients (PA and PB). Mitochondria in the fibroblasts and iPSCs from both groups showed long, cylindrical profiles with well-organized cristae, and the electron density of the matrix was relatively low (asterisks). Scale bar, 0.25 μm. Cont A, Control A; Cont B, Control B. (C) Fibroblasts were treated with 30μM CCCP or DMSO for 48 h, followed by staining for CIII corel (magenta) to label the internal mitochondrial membrane (IMM) and counterstaining with Hoechst (Ho, blue). Mitochondrial size decreased after CCCP treatment in both Control (Cont A and Cont B) and PARK2 (PA and PB) fibroblasts. Scale bar, 20 μm. (D) iPSCs were treated with 30 μM CCCP or DMSO for 48 h and then stained for CIII corel (magenta) to label IMM, Oct4 (blue) to label iPSCs, and Hoechst (Ho, white). Mitochondrial size in Control (Cont A (B7), Cont B (WD39)), and PARK2 (PA9 and PB2) iPSCs decreased after CCCP treatment. Scale bar, 20 μm (E) CCCP/DMSO ratios in Control (Cont A (B7, YA9), Cont B (WD39)), and PARK2 (PA9 and 22 and PB2 and 20) iPSCs (Mann Whitney *U*-test). Data represent the mean and SEM ($n > 3$ for each group).

Additional file 6: Mitochondrial membrane potential after CCCP treatment in control and PARK2 iPSC-derived neurons. (A) iPSC-derived neurons were treated with 30 μM CCCP or DMSO for 48 h, after which they were stained for the mitochondrial membrane potential marker, TMRE. The intensity of TMRE (yellow) was clearly reduced in

control (Cont A (B7), Cont B (WD39)), and PARK2 (PA9 and PB2) iPSC-derived neurons. Scale bar, 50 μm.

Additional file 7: Confirmation of *parkin* deletions carried by the father of patient PB. (A) Deletion of exons 6 and 7 was confirmed in blood samples from PB and the father of PB by PCR.

Additional file 8: α-Synuclein signals are not seen in PARK2 iPSCs. (A) Quantitative genomic PCR analysis for SNCA exons 1 and 4 demonstrated a normal copy number in PARK2 (PA1, 9 and 22, and PB1, 2, 18 and 20) iPSCs. The copy number was the same as that observed for Cont A (B7 and YA9) and Cont B (WD39). The *SNCA* gene copy number was normalized to β-globin *(HBB)* and β2-microglobulin *(B2MG)*. (B) iPSCs were stained for α-synuclein (red), Oct4 (green; to label iPSCs) and Hoechst (blue). No α-synuclein signals were observed in Cont A (B7 and YA9), Cont B (WD39), or PARK2 (PA9 and 22, PB2 and 20) iPSCs. Scale bar, 50 μm.

Competing interests
The authors declare that they have no competing interests.

Authors' contributions
YI, YO, WA, and HO conceived and designed the experiments. YI performed most of the experiments, analyzed data, and wrote the manuscript. YO, and HO edited the manuscript. YO developed the quality control system, neural differentiation method for the iPSCs and performed CGH microarray data analysis. WA generated the WD39 iPSCs. NK, KH, MS and AN performed western blotting analysis. TN performed some parts of *in vitro* culture assay. SS, MF, YM, HM and NH examined and recruited PARK2 patients. TK, MO, and MA performed biopsies and established the skin fibroblasts. AH, TS, TH and MS performed preliminary experiments for the metabolome analysis. TY, DI, AK and NS provided cent8-1 iPSCs. YI and NM designed the CCCP treatment experiment. MK and YU performed the electron microscopic analysis. HH, MT, HM and NH performed the histopathological studies of the postmortem brain of PA. All authors read and approved the final manuscript.

Acknowledgments
We would like to thank S. Yamanaka (CiRA) for the 201B7 iPSCs; N. Nakatsuji (Kyoto University) for the KhES cells; N. Izawa, S. Banno, Y. Matsuzaki, M. Fujiwara, Y. Nagahata, N. Hirose (Keio University), C. Kishi (Tokyo Medical and Dental University), M. Ogino, S. Miyakawa, (Kitasato University) and G. Takata (GE Healthcare Biosciences) for technical assistance and suggestions. This work was supported by the Project for the Realization of Regenerative Medicine and Support for the Core Institutes for iPS cell research from the Japanese Ministry of Education, Culture, Sports, Science and Technology (MEXT) to H.O., Exploratory Research for Advanced Technology (ERATO), Suematsu Gas Biology Project from Japan Science and Technology Agency (JST) to M.S., a Grant-in-Aid from the Japan Society for the Promotion of Science (JSPS) to W.A. and Y.O., the Keio Kanrinmaru Project and a Grant-in-Aid for Scientific Research on Innovative Areas to Y.O., a Grant-in-Aid for Scientific Research on Innovative Areas (Comprehensive Brain Science Network) from the MEXT to Y. O. and Y. I., a Grant-in-Aid for Encouragement of Young Medical Scientists from Keio University and the Japan Society for the Promotion of Science Fellows to Y.I., and a Grant-in-Aid for the Global COE Program at Keio University.

Author details
[1]Department of Physiology, Keio University School of Medicine, 35 Shinanomachi, Shinjuku-ku, Tokyo 160-8582, Japan. [2]Kanrinmaru Project, Keio University School of Medicine, Tokyo, Japan. [3]Department of Cell Biology and Neuroscience, Juntendo University Graduate School of Medicine, Tokyo, Japan. [4]Department of Neurology, Kitasato University School of Medicine, Kanagawa, Japan. [5]Department of Dermatology, Keio University School of Medicine, Tokyo, Japan. [6]Department of Neurology, Juntendo University School of Medicine, Tokyo, Japan. [7]Research Institute for Diseases of Old Age, Graduate School of Medicine, Juntendo University, Tokyo, Japan. [8]Institute for Advanced Biosciences, Keio University, Yamagata, Japan. [9]Department of Biochemistry, Keio University School of Medicine, Tokyo, Japan. [10]Department of Neurology, Keio University School of Medicine, Tokyo, Japan. [11]Advanced Science Research Laboratories, Pharmaceutical Research Division, Takeda Pharmaceutical Company Limited, Kanagawa, Japan. [12]Department of Neuro-Regenerative Medicine, Kitasato University School of Medicine, Kanagawa, Japan. [13]Department of Physiology and Cell Biology, Tokyo Medical and Dental University, Tokyo, Japan. [14]Department of Neurology, Osaka University Graduate School of Medicine, Osaka, Japan.

Received: 19 September 2012 Accepted: 2 October 2012
Published: 6 October 2012

References
1. Farrer MJ: **Genetics of Parkinson disease: paradigm shifts and future prospects.** *Nature reviews* 2006, **7**:306–318.
2. Kitada T, Asakawa S, Hattori N, Matsumine H, Yamamura Y, Minoshima S, Yokochi M, Mizuno Y, Shimizu N: **Mutations in the parkin gene cause autosomal recessive juvenile parkinsonism.** *Nature* 1998, **392**:605–608.
3. Shimura H, Hattori N, Kubo S, Mizuno Y, Asakawa S, Minoshima S, Shimizu N, Iwai K, Chiba T, Tanaka K, Suzuki T: **Familial Parkinson disease gene product, parkin, is a ubiquitin-protein ligase.** *Nat Genet* 2000, **25**:302–305.
4. Whitworth AJ, Pallanck LJ: **The PINK1/Parkin pathway: a mitochondrial quality control system?** *J Bioenerg Biomembr* 2009, **41**:499–503.
5. Youle RJ, Narendra DP: **Mechanisms of mitophagy.** *Nat Rev Mol Cell Biol* 2011, **12**:9–14.
6. Goldberg MS, Fleming SM, Palacino JJ, Cepeda C, Lam HA, Bhatnagar A, Meloni EG, Wu N, Ackerson LC, Klapstein GJ, *et al*: **Parkin-deficient mice exhibit nigrostriatal deficits but not loss of dopaminergic neurons.** *J Biol Chem* 2003, **278**:43628–43635.
7. Palacino JJ, Sagi D, Goldberg MS, Krauss S, Motz C, Wacker M, Klose J, Shen J: **Mitochondrial dysfunction and oxidative damage in parkin-deficient mice.** *J Biol Chem* 2004, **279**:18614–18622.
8. Perez FA, Palmiter RD: **Parkin-deficient mice are not a robust model of parkinsonism.** *Proc Natl Acad Sci USA* 2005, **102**:2174–2179.
9. Sato S, Chiba T, Nishiyama S, Kakiuchi T, Tsukada H, Hatano T, Fukuda T, Yasoshima Y, Kai N, Kobayashi K, *et al*: **Decline of striatal dopamine release in parkin-deficient mice shown by ex vivo autoradiography.** *J Neurosci Res* 2006, **84**:1350–1357.
10. Jiang H, Ren Y, Yuen EY, Zhong P, Ghaedi M, Hu Z, Azabdaftari G, Nakaso K, Yan Z, Feng J: **Parkin controls dopamine utilization in human midbrain dopaminergic neurons derived from induced pluripotent stem cells.** *Nat Commun* 2012, **3**:668.
11. Mattis VB, Svendsen CN: **Induced pluripotent stem cells: a new revolution for clinical neurology?** *Lancet Neurol* 2011, **10**:383–394.
12. Farrer M, Chan P, Chen R, Tan L, Lincoln S, Hernandez D, Forno L, Gwinn-Hardy K, Petrucelli L, Hussey J, *et al*: **Lewy bodies and parkinsonism in families with parkin mutations.** *Ann Neurol* 2001, **50**:293–300.
13. Savitt JM, Dawson VL, Dawson TM: **Diagnosis and treatment of Parkinson disease: molecules to medicine.** *J Clin Invest* 2006, **116**:1744–1754.
14. Ohta S, Imaizumi Y, Okada Y, Akamatsu W, Kuwahara R, Ohyama M, Amagai M, Matsuzaki Y, Yamanaka S, Okano H, Kawakami Y: **Generation of human melanocytes from induced pluripotent stem cells.** *PLoS One* 2011, **6**:e16182.
15. Takahashi K, Tanabe K, Ohnuki M, Narita M, Ichisaka T, Tomoda K, Yamanaka S: **Induction of pluripotent stem cells from adult human fibroblasts by defined factors.** *Cell* 2007, **131**:861–872.
16. Matigian N, Abrahamsen G, Sutharsan R, Cook AL, Vitale AM, Nouwens A, Bellette B, An J, Anderson M, Beckhouse AG, *et al*: **Disease-specific, neurosphere-derived cells as models for brain disorders.** *Dis Model Mech* 2010, **3**:785–798.
17. Nguyen HN, Byers B, Cord B, Shcheglovitov A, Byrne J, Gujar P, Kee K, Schule B, Dolmetsch RE, Langston W, *et al*: **LRRK2 mutant iPSC-derived DA neurons demonstrate increased susceptibility to oxidative stress.** *Cell Stem Cell* 2011, **8**:267–280.
18. Sies H: **Glutathione and its role in cellular functions.** *Free Radic Biol Med* 1999, **27**:916–921.
19. Williamson TP, Johnson DA, Johnson JA: **Activation of the Nrf2-ARE pathway by siRNA knockdown of Keap1 reduces oxidative stress and provides partial protection from MPTP-mediated neurotoxicity.** *Neurotoxicology* 2012, **33**:272–279.
20. Ramsey CP, Glass CA, Montgomery MB, Lindl KA, Ritson GP, Chia LA, Hamilton RL, Chu CT, Jordan-Sciutto KL: **Expression of Nrf2 in neurodegenerative diseases.** *J Neuropathol Exp Neurol* 2007, **66**:75–85.
21. Tufekci KU, Civi Bayin E, Genc S, Genc K: **The Nrf2/ARE Pathway: a promising target to counteract mitochondrial dysfunction in parkinson's disease.** *Parkinsons Dis* 2011, **2011**:314082.

22. Fukae J, Mizuno Y, Hattori N: **Mitochondrial dysfunction in Parkinson's disease.** *Mitochondrion* 2007, **7**:58–62.
23. Schapira AH: **Mitochondrial dysfunction in neurodegenerative disorders.** *Biochim Biophys Acta* 1998, **1366**:225–233.
24. Greene JC, Whitworth AJ, Kuo I, Andrews LA, Feany MB, Pallanck LJ: **Mitochondrial pathology and apoptotic muscle degeneration in Drosophila parkin mutants.** *Proc Natl Acad Sci USA* 2003, **100**:4078–4083.
25. Mortiboys H, Thomas KJ, Koopman WJ, Klaffke S, Abou-Sleiman P, Olpin S, Wood NW, Willems PH, Smeitink JA, Cookson MR, Bandmann O: **Mitochondrial function and morphology are impaired in parkin-mutant fibroblasts.** *Ann Neurol* 2008, **64**:555–565.
26. Matsuda N, Sato S, Shiba K, Okatsu K, Saisho K, Gautier CA, Sou YS, Saiki S, Kawajiri S, Sato F, *et al*: **PINK1 stabilized by mitochondrial depolarization recruits Parkin to damaged mitochondria and activates latent Parkin for mitophagy.** *J Cell Biol* 2010, **189**:211–221.
27. Narendra D, Tanaka A, Suen DF, Youle RJ: **Parkin is recruited selectively to impaired mitochondria and promotes their autophagy.** *J Cell Biol* 2008, **183**:795–803.
28. Tanaka A: **Parkin-mediated selective mitochondrial autophagy, mitophagy: Parkin purges damaged organelles from the vital mitochondrial network.** *FEBS Lett* 2010, **584**:1386–1392.
29. Yoshii SR, Kishi C, Ishihara N, Mizushima N: **Parkin mediates proteasome-dependent protein degradation and rupture of the outer mitochondrial membrane.** *J Biol Chem* 2011, **286**:19630–19640.
30. Seibler P, Graziotto J, Jeong H, Simunovic F, Klein C, Krainc D: **Mitochondrial Parkin recruitment is impaired in neurons derived from mutant PINK1 induced pluripotent stem cells.** *J Neurosci* 2011, **31**:5970–5976.
31. Shults CW: **Lewy bodies.** *Proc Natl Acad Sci USA* 2006, **103**:1661–1668.
32. Pramstaller PP, Schlossmacher MG, Jacques TS, Scaravilli F, Eskelson C, *Pepivani I, Hedrich K, Adel S, Gonzales-McNeal M, Hilker R, et al*: **Lewy body Parkinson's disease in a large pedigree with 77 Parkin mutation carriers.** *Ann Neurol* 2005, **58**:411–422.
33. Sasaki S, Shirata A, Yamane K, Iwata M: **Parkin-positive autosomal recessive juvenile Parkinsonism with alpha-synuclein-positive inclusions.** *Neurology* 2004, **63**:678–682.
34. Schlossmacher MG, Frosch MP, Gai WP, Medina M, Sharma N, Forno L, Ochiishi T, Shimura H, Sharon R, Hattori N, *et al*: **Parkin localizes to the Lewy bodies of Parkinson disease and dementia with Lewy bodies.** *Am J Pathol* 2002, **160**:1655–1667.
35. Chung KK, Zhang Y, Lim KL, Tanaka Y, Huang H, Gao J, Ross CA, Dawson VL, Dawson TM: **Parkin ubiquitinates the alpha-synuclein-interacting protein, synphilin-1: implications for Lewy-body formation in Parkinson disease.** *Nat Med* 2001, **7**:1144–1150.
36. Petrucelli L, O'Farrell C, Lockhart PJ, Baptista M, Kehoe K, Vink L, Choi P, Wolozin B, Farrer M, Hardy J, Cookson MR: **Parkin protects against the toxicity associated with mutant alpha-synuclein: proteasome dysfunction selectively affects catecholaminergic neurons.** *Neuron* 2002, **36**:1007–1019.
37. Shimura H, Schlossmacher MG, Hattori N, Frosch MP, Trockenbacher A, Schneider R, Mizuno Y, Kosik KS, Selkoe DJ: **Ubiquitination of a new form of alpha-synuclein by parkin from human brain: implications for Parkinson's disease.** *Science (New York, NY)* 2001, **293**:263–269.
38. Yagi T, Kosakai A, Ito D, Okada Y, Akamatsu W, Nihei Y, Nabetani A, Ishikawa F, Arai Y, Hirose N, *et al*: **Establishment of induced pluripotent stem cells from centenarians for neurodegenerative disease research.** *PLoS One* 2012, **7**:e41572.
39. Hargus G, Cooper O, Deleidi M, Levy A, Lee K, Marlow E, Yow A, Soldner F, Hockemeyer D, Hallett PJ, *et al*: **Differentiated Parkinson patient-derived induced pluripotent stem cells grow in the adult rodent brain and reduce motor asymmetry in Parkinsonian rats.** *Proc Natl Acad Sci USA* 2010, **107**:15921–15926.
40. Park IH, Arora N, Huo H, Maherali N, Ahfeldt T, Shimamura A, Lensch MW, Cowan C, Hochedlinger K, Daley GQ: **Disease-Specific Induced Pluripotent Stem Cells.** *Cell* 2008, .
41. Soldner F, Hockemeyer D, Beard C, Gao Q, Bell GW, Cook EG, Hargus G, Blak A, Cooper O, Mitalipova M, *et al*: **Parkinson's disease patient-derived induced pluripotent stem cells free of viral reprogramming factors.** *Cell* 2009, **136**:964–977.
42. Devine MJ, Ryten M, Vodicka P, Thomson AJ, Burdon T, Houlden H, Cavaleri F, Nagano M, Drummond NJ, Taanman JW, *et al*: **Parkinson's disease induced pluripotent stem cells with triplication of the alpha-synuclein locus.** *Nat Commun* 2011, **2**:440.
43. Suemori H, Yasuchika K, Hasegawa K, Fujioka T, Tsuneyoshi N, Nakatsuji N: **Efficient establishment of human embryonic stem cell lines and long-term maintenance with stable karyotype by enzymatic bulk passage.** *Biochem Biophys Res Commun* 2006, **345**:926–932.
44. Okada Y, Matsumoto A, Shimazaki T, Enoki R, Koizumi A, Ishii S, Itoyama Y, Sobue G, Okano H: **Spatiotemporal recapitulation of central nervous system development by murine embryonic stem cell-derived neural stem/progenitor cells.** *Stem cells (Dayton, Ohio)* 2008, **26**:3086–3098.
45. Koike M, Shibata M, Waguri S, Yoshimura K, Tanida I, Kominami E, Gotow T, Peters C, von Figura K, Mizushima N, *et al*: **Participation of autophagy in storage of lysosomes in neurons from mouse models of neuronal ceroid-lipofuscinoses (Batten disease).** *Am J Pathol* 2005, **167**:1713–1728.
46. Mitsui J, Takahashi Y, Goto J, Tomiyama H, Ishikawa S, Yoshino H, Minami N, Smith DI, Lesage S, Aburatani H, *et al*: **Mechanisms of genomic instabilities underlying two common fragile-site-associated loci, PARK2 and DMD, in germ cell and cancer cell lines.** *Am J Hum Genet* 2010, **87**:75–89.

doi:10.1186/1756-6606-5-35
Cite this article as: Imaizumi *et al.*: Mitochondrial dysfunction associated with increased oxidative stress and α-synuclein accumulation in PARK2 iPSC-derived neurons and postmortem brain tissue. *Molecular Brain* 2012 5:35.

Submit your next manuscript to BioMed Central and take full advantage of:

- Convenient online submission
- Thorough peer review
- No space constraints or color figure charges
- Immediate publication on acceptance
- Inclusion in PubMed, CAS, Scopus and Google Scholar
- Research which is freely available for redistribution

Submit your manuscript at
www.biomedcentral.com/submit

BioMed Central

Lewy Body Pathology in a Patient With a Homozygous *Parkin* Deletion

Saori Miyakawa, MD,[1]* Mieko Ogino, MD, PhD,[1]
Sayaka Funabe, MD,[2,3] Akiko Uchino, MD,[1]
Yasushi Shimo, MD, PhD,[2] Nobutaka Hattori, MD, PhD,[2]
Masaaki Ichinoe, MD, PhD,[4] Tetuo Mikami, MD, PhD,[4]
Makoto Saegusa, MD, PhD,[4] Kazutoshi Nishiyama, MD, PhD,[1] Hideo Mori, MD, PhD,[2] Yoshikuni Mizuno, MD, PhD,[5]
Shigeo Murayama, MD, PhD[3] and
Hideki Mochizuki, MD, PhD[6]

[1]Department of Neurology, Kitasato University School of Medicine, Kanagawa, Japan; [2]Department of Neurology, Juntendo University School of Medicine, Tokyo, Japan; [3]Department of Neuropathology, Tokyo Metropolitan Institute of Gerontology, Tokyo, Japan; [4]Department of Pathology, Kitasato University School of Medicine, Kanagawa, Japan; [5]Department of Neuroregenerative Medicine, Kitasato University School of Medicine, Kanagawa, Japan; [6]Department of Neurology, Osaka University School of Medicine, Osaka, Japan.

ABSTRACT

Background: We report neuropathologic findings in a patient with homozygous deletions of exons 2 to 4 of *parkin*.

Results: Although the absence of Lewy bodies has been considered a neuropathologic characteristic of *parkin* mutation, here we report a pathologic finding with the presence of Lewy bodies.

Methods: The patient was a 72-year-old woman with onset of the disease at age 61. Her autopsy revealed marked decrease in melanized neurons in the substantia nigra and the locus coeruleus. Lewy bodies were found in the substantia nigra, the locus coeruleus, the dorsal motor nucleus of the vagus, the basal nucleus of Meynert, the amygdaloid nucleus, and the sympathetic nerve bundles in the myocardium.

Conclusions: Only 3 previous case reports described Lewy body formation in patients carrying *parkin* mutations. The distribution of Lewy bodies in our patient appeared to be reminiscent of sporadic Parkinson's disease. © 2013 *Movement* Disorder Society

Key Words: PARK2; Lewy body; α-synuclein; parkin; neuropathology

Parkinsonism associated with *parkin* mutations (PARK2) is characterized by early onset (age < 40 years), slow progression, good response to levodopa, sleep benefit, levodopa-induced motor fluctuations, and dyskinesias.[1–5] Selective neuronal degeneration in the pigmented neurons of the substantia nigra (SN) without Lewy body formation is considered a pathologic characteristic of PARK2-linked Parkinson's disease (PD)[6–11]; however, Lewy body–positive cases have also been reported.[12–14] We had a chance to see an autopsied case of a PARK2 patient who had numerous Lewy bodies in the brain.

Case Report

The patient was a 72-year-old woman. She noted onset of difficulty in walking in her left leg at age 61. At age 64, difficulty in walking spread to her right leg with start hesitation. She was seen at Juntendo University Hospital on December 13, 2001. She showed tremor in her left hand, mild rigidity, bradykinesia, gait disturbance, and postural instability. Her parents were first cousins. Her mother was said to have PD, but the details were not clear. Her father did not have PD.

Her brain MRI was unremarkable. Cardiac MIBG scintigraphy at age 66 was normal (heart-to-mediastinum uptake ratio was 2.27 in the early phase and 2.14 in the delayed phase; normal value for the institute, >1.45). Genetic analysis revealed homozygous deletions of exons 2–4 of *parkin*.

She was at Yahr stage I to II with cabergoline. At age 67, levodopa/carbidopa was started because of postural instability. She had no orthostatic hypotension or dementia. She began to have wearing-off and dyskinesia at age 68. She received bilateral STN-DBS at age 71 with improvement in her motor fluctuation. At age 72, she was admitted to our hospital because of severe pneumonia. Shortly after admission, her clinical status deteriorated, and she died of respiratory failure. Autopsy was performed 2 hours after death.

*Correspondence to: Dr. Saori Miyakawa, Department of Neurology, Kitasato University, School of Medicine, 1-15-1 Kitasato, Minami-ku, Sagamihara, Kanagawa, 252-0374, Japan; saomiya@med.kitasato-u.ac.jp

Relevant conflicts of interest/financial disclosures: Yoshikuni Mizuno is a professor of a department that was donated by Boehlinger-Ingelheim, Japan, Inc., and Medotronics, Japan, Inc.

Full financial disclosures and author roles may be found in the online version of this article.

Received: 13 August 2012; **Revised:** 25 November 2012; **Accepted:** 29 November 2012
Published online 11 February 2013 in Wiley Online Library (wileyonlinelibrary.com).
DOI: 10.1002/mds.25346

Neuropathologic Findings

The brain samples were embedded in paraffin, and sections 4 μm thick were made. They were stained with hematoxylin-eosin (HE), Klüver-Barrera, and Gallyas-Braak and immunostained with the following antibodies: antiphosphorylated α-synuclein (psyn #64, Dako, Kyoto, Japan), antiphosphorylated tau (AT8; Innogenetics, Temse, Belgium), and anti–amyloid-beta protein (11-28; IBL, Fujioka, Japan). The anterior walls of the left ventricles of the hearts of this patient, a patient with sporadic PD, and a control patient were stained with HE and immunostained with psyn #64, antityrosine hydroxylase (TH; Calbiochem, Darmstadt, Germany), and antiphosphorylated neurofilament (SMI31; Sternberger Immunochemicals, Bethesda, MD). Brains of the 3 patients with PD and dementia (PDD) were also stained for α-synuclein pathology for comparison.

The weight of the brain was 1260 g with no atrophy. The serial coronal sections of the brain and horizontal sections of the brain stem showed severe loss of pigmentation in the SN (Fig. 1a) and locus coeruleus (LC; Fig. 1b). Microscopically, the numbers of melanin-containing neurons were decreased in the SN (Fig. 1c) and LC. Lewy bodies were seen in the SN (Fig. 1c) and LC. Immunostaining with psyn #64 showed Lewy bodies and Lewy neuritis in the remaining neurons of the SN, LC (Fig. 1d), dorsal motor nucleus of the vagus (Fig. 1e), amygdaloid nucleus, basal nucleus of Meynert (nbM; Fig. 1f), striatum, and anterior cingulate cortex. Semiquantitative observation of Lewy-related pathology in 3 sporadic PD patients based on the scoring system of the Third Report of the DLB Consortium[15] revealed 3 (severe) in the SN and nbM in all 3 patients, and 3.7 ± 0.58 (4 [very severe], 4, and 3) in the amygdaloid nucleus (central), although in our patient, it was 3 in the SN, nbM, and amygdaloid nucleus (central). From the distribution of Lewy bodies, her brain corresponded to stage IV of Braak's classification.[16] Tau-positive inclusions were observed only in the entorhinal cortex. β-Amyloid plaques were absent.

Lewy bodies were also found in the adrenal medulla (Fig. 1g). The nerve fibers in the epicardium were shown to contain eosinophilic inclusions with HE staining, which were recognized by immunostaining with psyn #64 (Fig. 1h). Immunostaining for TH of the nerve fibers in the epicardium showed intense staining in the control patient, no immunostaining in the patient with sporadic PD, and intermediate staining in this patient. Immunostaining with phosphorylated neurofilament in the nerve fibers of the epicardium was the same intensity as the staining with TH immunostaining, indicating intermediate degeneration of the cardiac sympathetic nerve bundles.

Discussion

We have reported the pathology of a patient with homozygous deletions of exons 2–4 of *parkin* who had Lewy bodies in many areas of the brain. Until now, 3 cases of PARK2 with Lewy bodies have been reported in the literature (Table 1).[12–14] The case reported by Farrer et al was a man who had onset of the disease at age 41 and died at age 52.[12] He had compound heterozygous mutations of *parkin* (R275W at exon 7 and 40-base-pair deletion in exon 3). Loss of pigmented neurons and Lewy bodies were seen in the SN and LC. Immunostaining for α-synuclein revealed no Lewy bodies in other areas of the brain, except for a few Lewy bodies in the nbM and the amygdala-parahippocampal region and the occasional Lewy neurites in the dorsal motor nucleus of the vagus. Farrer et al stated that their case did not differ in any respect from that seen in mild to moderate idiopathic PD. The case reported by Sasaki et al was a woman who had onset of the disease at age 33 and died at age 70.[13] She had homozygous deletion of exon 3 in *parkin*. There was moderate loss of pigmented neurons in the SN and LC. Lewy bodies were not observed in the SN or the LC. Inclusion bodies resembling Lewy bodies but more basophilic were noted in the neuropil of the pedunculopontine nucleus. The case reported by Pramstaller et al was a man who had onset of the disease at age 49 and died at age 73.[14] Marked loss of neurons was found in the SN and LC. A small number of Lewy bodies were seen in the SN and LC. They could detect truncated Parkin protein in the SN of this patient. The presence of truncated Parkin may be a reason for the presence of Lewy bodies in our case. We confirmed the absence of full-length *parkin* in our case; however, the presence of truncated Parkin cannot be excluded completely.

Thus, the case reported by Farrer et al[12] is similar to our case, and the case reported by Parmstaller et al[14] has some resemblance, even though the number of Lewy bodies was smaller. In our patient, Lewy bodies were detected in many areas of the brain. This distribution of Lewy bodies may well be seen in sporadic PD. Until now 9 cases of autopsied PARK2 patients have been reported including ours,[7–14] of which 4 cases including ours had Lewy bodies.[12–14]

Cardiac uptake of ^{123}I-MIBG scintigraphy was normal in our case 5 years after onset when the patient was in stage III of Hoehn and Yahr. Pathological examination showed relatively preserved sympathetic nerve fibers in the epicardium compared with patients with sporadic PD.[17] But Lewy body formation was found in the epicardial nerve fibers. According to the literature, cardiac TH-positive fibers show marked degeneration in sporadic PD with α-synuclein deposition,[17] whereas TH-positive fibers were retained in PARK2.[18] In our patient, TH-positive fibers and epicardial axonal fibers

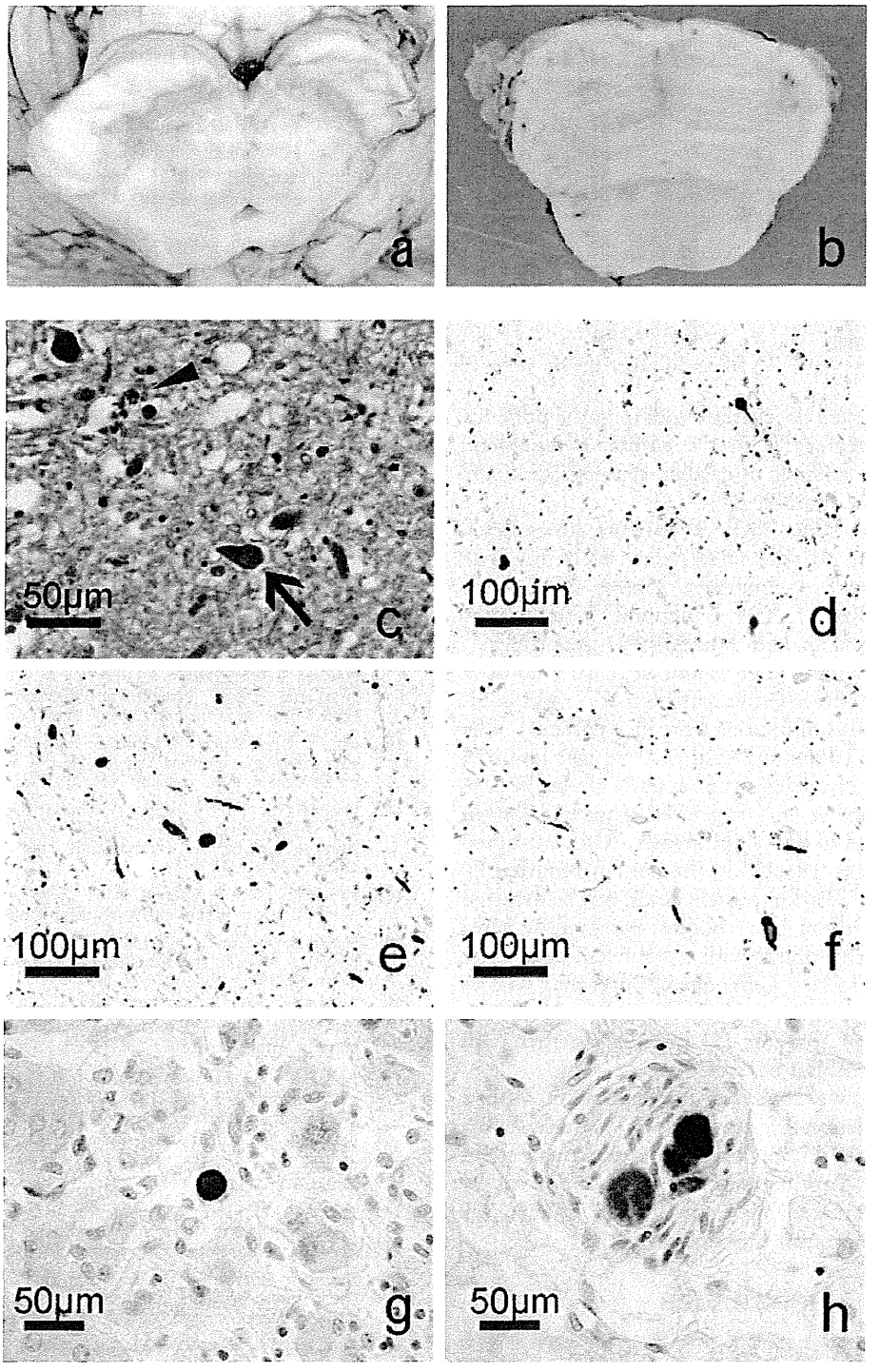

FIG. 1. Neuropathologic findings of the patient. The substantia nigra shows marked depigmentation in the macroscopic view (**a**). HE staining of the substantia nigra shows a Lewy body (arrow) in the remaining neuron (**c**), severe loss of pigmented neurons, and melanophagia (arrowhead). The locus coeruleus cannot be identified because of severe depigmentation in the macroscopic view (**b**). Immunostaining for α-synuclein shows a Lewy body in the remaining neurons and Lewy neuritis in the LC (**d**). Immunostaining for α-synuclein in the dorsal motor nucleus of the vagus (**e**), and the nbM (**f**) shows Lewy bodies and Lewy neuritis. The adrenal medulla also shows Lewy bodies by α-synuclein immunostaining (**g**). Immunostaining for α-synuclein of the nerve fibers in the epicardium shows Lewy bodies (**h**).

TABLE 1. Summary of Lewy body–positive and –negative cases of PARK2

	Sex	Age at onset	Age at death	Mutation	LB distribution
Lewy body–positive cases of PARK2					
Farrer et al, 2001	M	41	52	R275W, del 40 bp in Exon3	Transitional
Sasaki et al, 2004	F	33	70	Homozygous delExon3	Pedunculopontine
Pramistaller et al, 2005	M	49	73	delExon7, del1072T	Brain stem
Our patient	F	61	72	Homozygous delExon2–4	Transitional
Lewy body–negative cases of PARK2					
Yamamura et al, 1998	F	20	52	delExon3, delExon3	No LB
Mori et al, 1998	M	24	62	Homozygous delExon4	No LB
Hayashi et al, 2000	M	32	70	Homozygous delExon4	No LB
van de Warrenburg et al, 2001	M	18	75	Lys211Asn, delExon3	No LB
Gouider-Khouja et al, 2003	M	34	47	Homozygous dlbp101–102 in Exon2	No LB

did not show marked degeneration, despite the presence of α-synuclein aggregates in the cardiac sympathetic nerve fibers. The findings of cardiac sympathetic fibers were not typical of sporadic PD.

Then, why do some PARK2 patients have Lewy bodies and others do not? There seems to be no clear relation to the type of mutation. Among the 4 cases with Lewy bodies, 2 had compound heterozygous mutations[12,14] and 2 had homozygous mutations.[13] Homozygous deletions were found in 4 of 5 autopsy cases of Lewy body–negative patients,[7–9,11] and compound heterozygous mutations were in 1 patient.[10] The case reported by Yamamura et al in 1998 was reported to have homozygous deletions of exon 3.[6,19] In the case reported by Farrer et al,[12] expressed truncated Parkin protein was found in the lymphoblasts. Also, truncated Parkin protein was detected in the patient reported by Pramstaller et al.[14] Parkin protein could not be detected in the patient (without Lewy bodies) reported by Mori et al.[8,20] Parkin colocalizes with α-synuclein aggregates in Lewy bodies of PD.[21] Older age of onset may well be a reason for the positivity of Lewy bodies. However, the coexistence of sporadic PD process together with *parkin* mutation cannot be excluded.

In conclusion, we have reported a patient with a homozygous deletion of *parkin* who showed many Lewy bodies in the brain. We believe that this patient started with a Parkin-deficient brain followed by sporadic PD changes; however, further studies are necessary to explore this question. ■

References

1. Yamamura Y, Sobue I, Ando K, et al. Paralysis agitans of early onset with marked diurnal fluctuation of symptoms. Neurology 1973;23:239–244.
2. Ishikawa A, Tsuji S. Clinical analysis of 17 patients in 12 Japanese families with autosomal-recessive type juvenile parkinsonism. Neurology 1996;47:160–169.
3. Kitada T, Asakawa S, Hattori N, et al. Mutations in the parkin gene cause autosomal recessive juvenile parkinsonism. Nature 1998;392:605–608.
4. Lücking CB, Dürr A, Bonifati V, et al. Association between early-onset Parkinson's disease and mutations in the parkin gene. N Engl J Med 2000;342:1560–1567.
5. Periquet M, Latouche M, Lohmann E, et al. Parkin mutations are frequent in patients with isolated early-onset parkinsonism. Brain 2003;126:1271–1278.
6. Poulopoulos M, Levy OA, Alcalay RN. The neuropathology of genetic Parkinson's disease. Mov Disord 2012;27:831–842.
7. Yamamura Y, Kuzuhara S, Kondo K, et al. Clinical, pathologic and genetic studies on autosomal recessive early-onset parkinsonism with diurnal fluctuation. Parkinsonism Relat Disord 1998;4:65–72.
8. Mori H, Kondo T, Yokochi M, et al. Pathologic and biochemical studies of juvenile parkinsonism linked to chromosome 6q. Neurology 1998;51:890–892.
9. Hayashi S, Wakabayashi K, Ishikawa A, et al. An autopsy case of autosomal-recessive juvenile parkinsonism with a homozygous exon 4 deletion in the parkin gene. Mov Disord 2000;15:884–888.
10. van de Warrenburg BP, Lammens M, Lücking CB, et al. Clinical and pathologic abnormalities in a family with parkinsonism and parkin gene mutations. Neurology 2001;56:555–557.
11. Gouider-Khouja N, Larnaout A, Amouri R et al. Autosomal recessive parkinsonism linked to parkin gene in a Tunisian family. Clinical, genetic and pathological study. Parkinsonism Relat Disord 2003;9:247–251.
12. Farrer M, Chan P, Chen R, et al. Lewy bodies and parkinsonism in families with parkin mutations. Ann Neurol 2001;50:293–300.
13. Sasaki S, Shirata A, Yamane K, et al. Parkin-positive autosomal recessive juvenile parkinsonism with α-synuclein-positive inclusions. Neurology 2004;63:678–682.
14. Pramstaller PP, Schlossmacher MG, Jacques TS, et al. Lewy body Parkinson's disease in a large pedigree with 77 parkin mutation carriers. Ann Neurol 2005;58:411–22.
15. McKeith IG, Dickson DW, Lowe J, et al. Diagnosis and management of dementia with Lewy bodies. Third Report of the DLB Consortium. Neurology 2005;65:1863–1872.
16. Braak H, Tredici KD, Rub U, et al. Staging of brain pathology related to sporadic Parkinson's disease. Neurobiol Aging 2003;24:197–211.
17. Orimo S, Uchihara T, Nakamura A, et al. Axonal α-synuclein aggregates herald centripetal degeneration of cardiac sympathetic nerve in Parkinson's disease. Brain 2008;131:642–650.
18. Orimo S, Amino T, Yokochi M, et al. Preserved cardiac sympathetic nerve accounts for normal cardiac uptake of MIBG in PARK2. Mov Disord 2005;20:1350–1353.
19. Yamamura Y, Hattori N, Matsumine H, et al. Autosomal recessive early-onset parkinsonism with diurnal fluctuation: clinicopathologic characteristics and molecular genetic identification. Brain Dev 2000;22:S87–S91.
20. Shimura H, Hattori N, Kubo S, et al. Immunohistochemical and subcellular localization of Parkin: absence of protein in autosomal recessive juvenile parkinsonism patients. Ann Neurol 1999;45:668–672.
21. Schlossmacher MG, Frosch MP, Gai WP, et al. Parkin localizes to the Lewy bodies of Parkinson disease and dementia with Lewy bodies. Am J Pathol 2002;160:1655–1667.

nature COMMUNICATIONS

ARTICLE

Received 17 Sep 2012 | Accepted 20 Dec 2012 | Published 29 Jan 2013

DOI: 10.1038/ncomms2417

Heat shock factor-1 influences pathological lesion distribution of polyglutamine-induced neurodegeneration

Naohide Kondo[1], Masahisa Katsuno[1], Hiroaki Adachi[1], Makoto Minamiyama[1], Hideki Doi[1], Shinjiro Matsumoto[1], Yu Miyazaki[1], Madoka Iida[1], Genki Tohnai[1], Hideaki Nakatsuji[1], Shinsuke Ishigaki[1], Yusuke Fujioka[1], Hirohisa Watanabe[1], Fumiaki Tanaka[1], Akira Nakai[2] & Gen Sobue[1]

A crucial feature of adult-onset neurodegenerative diseases is accumulation of abnormal protein in specific brain regions, although the mechanism underlying this pathological selectivity remains unclear. Heat shock factor-1 is a transcriptional regulator of heat shock proteins, molecular chaperones that abrogate neurodegeneration by refolding and solubilizing pathogenic proteins. Here we show that heat shock factor-1 expression levels are associated with the accumulation of pathogenic androgen receptor in spinal and bulbar muscular atrophy, a polyglutamine-induced neurodegenerative disease. In heterozygous *heat shock factor-1*-knockout spinal and bulbar muscular atrophy mice, abnormal androgen receptor accumulates in the cerebral visual cortex, liver and pituitary, which are not affected in their genetically unmodified counterparts. The depletion of *heat shock factor-1* also expands the distribution of pathogenic androgen receptor accumulation in other neuronal regions. Furthermore, lentiviral-mediated delivery of heat shock factor-1 into the brain of spinal and bulbar muscular atrophy mice topically suppresses the pathogenic androgen receptor accumulation and neuronal atrophy. These results suggest that heat shock factor-1 influences the pathological lesion selectivity in spinal and bulbar muscular atrophy.

[1] Department of Neurology, Nagoya University Graduate School of Medicine, Nagoya 466-8550, Japan. [2] Department of Biochemistry and Molecular Biology, Yamaguchi University School of Medicine, Ube 755-8505, Japan. Correspondence and requests for materials should be addressed to M.K. (email: ka2no@med.nagoya-u.ac.jp).

© 2013 Macmillan Publishers Limited. All rights reserved.